

Low-pressure–high-temperature metamorphism during extension in a Jurassic magmatic arc, Central Pontides, Turkey

A. I. OKAY,^{1,2} G. SUNAL,² O. TÜYSÜZ,^{1,2} S. SHERLOCK,³ M. KESKIN⁴ AND A. R.C. KYLANDER-CLARK⁵

¹Eurasia Institute of Earth Sciences, Istanbul Technical University, Maslak, 34469, Turkey (okay@itu.edu.tr)

²Department of Geology, Faculty of Mines, Istanbul Technical University, Maslak, 34469, Turkey

³Department of Earth, Environment and Ecosystems, Centre for Earth, Planetary, Space & Astronomical Research (CEPSAR) Sciences, The Open University, Walton Hall, Milton Keynes, MK7 6AA, UK

⁴Department of Geological Engineering, Istanbul University, Avcılar, 34320, Istanbul, Turkey

⁵Department of Earth Sciences, University of California Santa Barbara, Santa Barbara, CA, 93106, USA

ABSTRACT Magmatic arcs are zones of high heat flow; however, examples of metamorphic belts formed under magmatic arcs are rare. In the Pontides in northern Turkey, along the southern active margin of Eurasia, high temperature–low pressure metamorphic rocks and associated magmatic rocks are interpreted to have formed under a Jurassic continental magmatic arc, which extends for 2800 km through the Crimea and Caucasus to Iran. The metamorphism and magmatism occurred in an extensional tectonic environment as shown by the absence of a regional Jurassic contractional deformation, and the presence of Jurassic extensional volcanoclastic marine basin in the Pontides, over 2 km in thickness, where deposition was coeval with the high-*T* metamorphism at depth. The heat flow was focused during the metamorphism, and unmetamorphosed Triassic sequences crop out within a few kilometres of the Jurassic metamorphic rocks. The heat for the high-*T* metamorphism was brought up to crustal levels by mantle melts, relicts of which are found as ultramafic, gabbroic and dioritic enclaves in the Jurassic granitoids. The metamorphic rocks are predominantly gneiss and migmatite with the characteristic mineral assemblage quartz + K-feldspar + plagioclase + biotite + cordierite ± sillimanite ± garnet. Mineral equilibria give peak metamorphic conditions of 4 ± 1 kbar and 720 ± 40 °C. Zircon U–Pb and biotite Ar–Ar ages show that the peak metamorphism took place during the Middle Jurassic at *c.* 172 Ma, and the rocks cooled to 300 °C at *c.* 162 Ma, when they were intruded by shallow-level dacitic and andesitic porphyries and granitoids. The geochemistry of the Jurassic porphyries and volcanic rocks has a distinct arc signature with a crustal melt component. A crustal melt component is also suggested by cordierite and garnet in the magmatic assemblage and the abundance of inherited zircons in the porphyries.

Key words: extension; LP–HT metamorphism; magmatic arc; Pontides; Turkey.

INTRODUCTION

Low pressure–high temperature (LP–HT) metamorphic rocks are generally characterized by the presence of cordierite and sillimanite, by partial melting, and by association with syn- to post-tectonic plutonic rocks (e.g. Barton & Hanson, 1989; Deyoreo *et al.*, 1991). Three tectonic environments are generally invoked for their generation (e.g. Craven *et al.*, 2012): (i) A thickened orogen, which extends by gravitational collapse, owing to the removal of lower crustal or lithospheric mantle. (ii) A continental rift zone. (iii) Mid-crustal levels of a magmatic arc. Each of these settings will have its individual signature in the regional geology and in the *P–T* paths of the metamorphic rocks. In the first tectonic setting, crustal thickening precedes the extension, whereas in the second and third cases an initially thick crust is not a pre-requisite.

Most LP–HT metamorphic belts show an early high- to medium-pressure metamorphism, which indicates an initial period of crustal thickening (e.g. Vissers, 1992; Amato *et al.*, 1994; Gardien *et al.*, 1997; Platt *et al.*, 2003), and points to a setting in a collisional orogenic belt. In such settings, the magmatism may be caused by the upward flow of the hot asthenosphere into the space created by the removal of the lower crust and/or lithospheric mantle. LP–HT metamorphism in rift zones without a prior orogenic activity is apparently rare. It was suggested for the Pyrenees (Wickham & Oxburgh, 1985), however, subsequent studies have generally demonstrated the presence of an earlier episode of crustal thickening. LP–HT metamorphic belts related unambiguously to magmatic arcs are also rare with a few examples reported from the Andes (e.g. Lucassen & Franz, 1996). Here, Jurassic LP–HT regional metamorphism and associated acidic to intermediate magmatism are

described from the Pontides in northern Turkey, which we suggest took place in the mid-crustal levels of an extensional continental magmatic arc. The Jurassic volcanic arc extends from the Crimea through the Central and Eastern Pontides to the Caucasus and farther east to Iran. Most of it consists of sedimentary and volcanic rocks, which allows a precise correlation between sedimentation, volcanism and metamorphism.

The second aim of the paper was to contribute to the Jurassic tectonics of the Black Sea region. Although Jurassic volcanic and subvolcanic rocks are widely described from the margins of the eastern Black Sea, LP–HT Jurassic regional metamorphism was previously unknown. The presence of Jurassic LP–HT metamorphism in the Pontides reinforces the view of the Pontides as the south-facing active margin of Eurasia during the Mesozoic.

GEOLOGICAL SETTING

The Pontides are the mountain chain between the Black Sea in the north and the İzmir–Ankara suture in the south (Fig. 1). During the Mesozoic, the Pontides constituted part of the active margin of Eurasia facing a wide Tethyan ocean in the south. The Tethys was finally consumed in the early Tertiary, resulting in the collision of the Pontides with the Anatolide–Tauride Block (e.g. Şengör & Yılmaz, 1981; Okay & Tüysüz, 1999).

The Pontides consist of three terranes, which are the Sakarya and İstanbul zones, and the Strandja Massif (Fig. 1). Central Pontides is a geographic term describing the northward arched section of the Pontide mountain chain. It includes two of the Pontic

terrane: the İstanbul Zone in the west and the Sakarya Zone in the east. In the Central Pontides, the İstanbul and Sakarya zones have a common post-Upper Jurassic stratigraphy but differ in their earlier geological histories (Fig. 2). The İstanbul Zone has a Neoproterozoic crystalline basement overlain by a Palaeozoic series including Carboniferous coal measures (e.g. Görür *et al.*, 1997; Dean *et al.*, 2000; Chen *et al.*, 2002; Özgül, 2012). The Palaeozoic sedimentary rocks are intruded by Permian granitoids and are unconformably overlain by Permo-Triassic terrigenous sedimentary rocks. A Middle Jurassic continental to shallow marine sedimentary sequence occurs locally between the Permo-Triassic red beds and the Upper Jurassic limestones (Maden Tetkik ve Arama Enstitüsü, 1974; Derman *et al.*, 1995).

In the Central Pontides, the Sakarya Zone has a Hercynian metamorphic-granitic basement with Late Carboniferous–Early Permian granitoids (Nzegge *et al.*, 2006). The Triassic sequence, called the Küre Complex, comprises a thick Upper Triassic flysch series with basalt and dolerite flows (Ustaömer & Robertson, 1994), which are intruded by Middle Jurassic granitoids (Yılmaz & Boztuğ, 1986). Both the Sakarya- and İstanbul-type sequences are unconformably overlain by Upper Jurassic–Lower Cretaceous shallow marine carbonates locally with basal continental clastics (Fig. 2, Tüysüz, 1990; Yiğitbaş *et al.*, 1999). A thick siliciclastic Lower Cretaceous turbidite sequence, the Çağlayan Formation, lies unconformably over the carbonates, as well as over the older formations (Fig. 3, Tüysüz, 1999; Hippolyte *et al.*, 2010).

The southern part of the Central Pontides consists predominantly of metamorphic rocks, long consid-

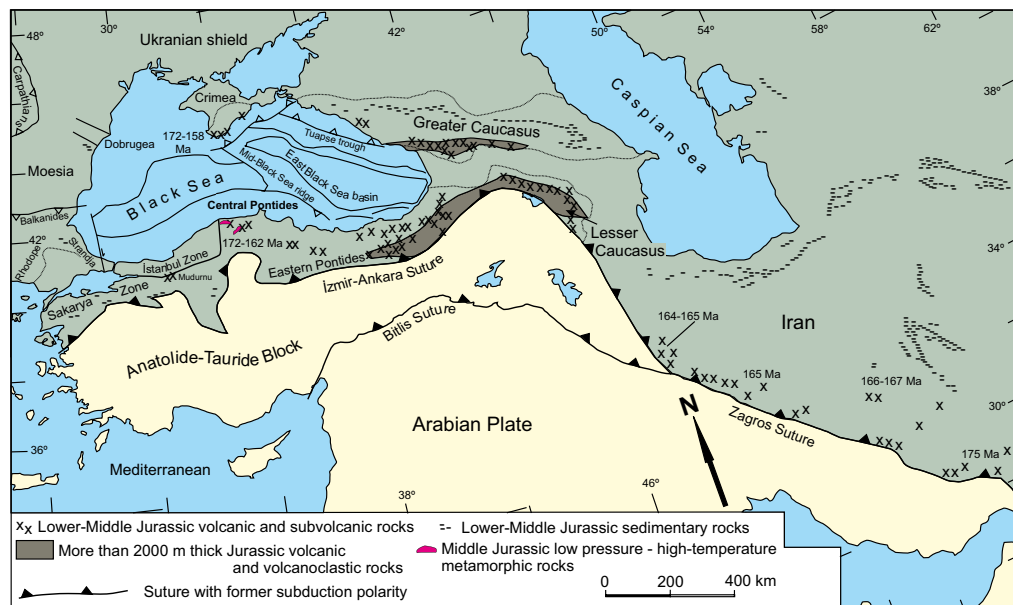


Fig. 1. Tectonic map of the Eastern Mediterranean–Black Sea–Iran showing the Jurassic magmatic belt and Jurassic high-temperature metamorphic rocks in the Central Pontides. The isotopic ages are from Meijers *et al.* (2010), Chiu *et al.* (2013) and this study.

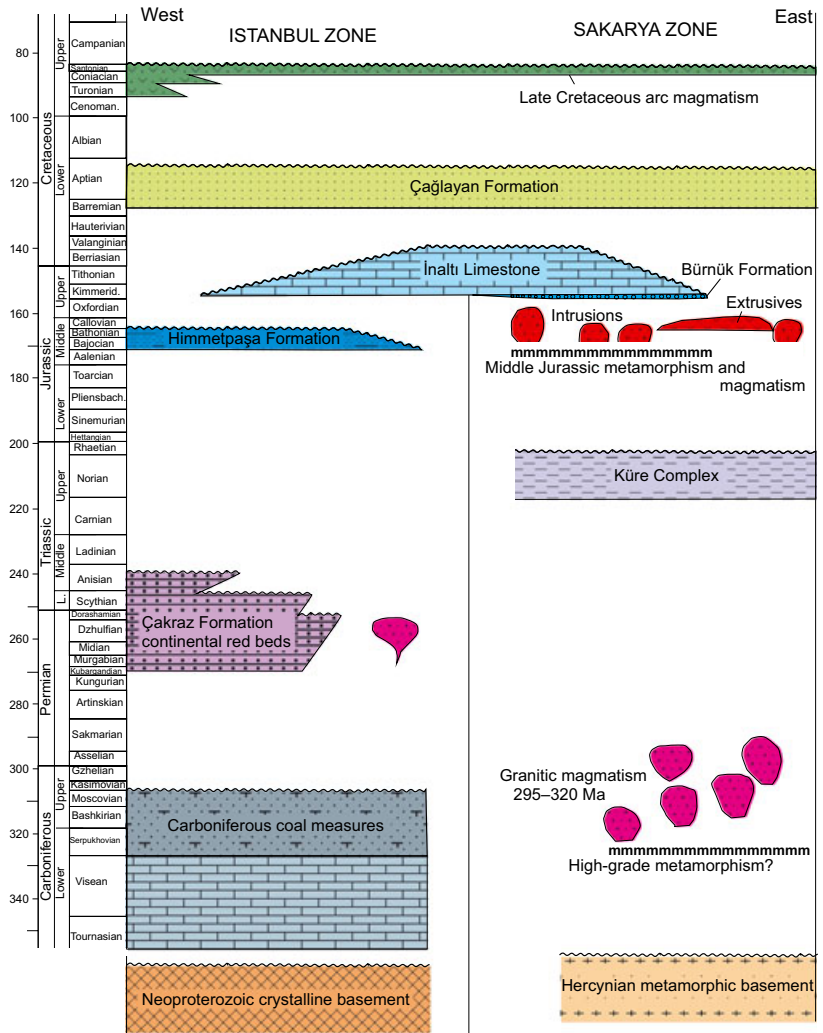


Fig. 2. Upper Palaeozoic–Mesozoic stratigraphy of the Central Pontides.

ered to be a pre-Triassic crystalline basement (Yılmaz & Şengör, 1985; Tüysüz, 1990; Ustaömer & Robertson, 1994, 1999; Yılmaz *et al.*, 1997; Uğuz *et al.*, 2002). However, recent data have shown that it consists of Early Cretaceous and Jurassic accretionary complexes, called collectively as the Central Pontide Supercomplex (Fig. 3, Okay *et al.*, 2006, 2013). The metamorphism is in eclogite, blueschist and high-pressure greenschist to amphibolite facies and is of Early Cretaceous and Middle Jurassic in age.

The Jurassic magmatism has a wide distribution in the Black Sea region extending for 2800 km from Iran through the Caucasus to the Pontides and Crimea (Fig. 1, Şengör *et al.*, 1991; Okay & Şahintürk, 1997; Meijers *et al.*, 2010; McCann *et al.*, 2010; Adamia *et al.*, 2011). Most of it is in the form of submarine lavas, tuffs and agglomerates, which are intercalated with shallow marine to continental clastic and epiclastic sedimentary rocks. In contrast, the Central Pontides expose a lower crustal level of the Jurassic magmatic belt with acidic to intermediate intrusions and associated high-temperature metamorphic rocks (Fig. 3).

MIDDLE JURASSIC LP-HT METAMORPHISM IN THE CENTRAL PONTIDES

In the Central Pontides, the Jurassic metamorphic rocks form two large metamorphic bodies, known as the Geme Complex in the north and the Devrekani Massif in south (Fig. 3). We have studied the Geme Complex in detail and the Devrekani Massif on a reconnaissance level.

The Geme Complex

The Geme Complex is an east–west-oriented metamorphic body close to the Black Sea coast, 25 km long and 5 km wide (Fig. 3). There is no previous published description of the Geme Complex. In the published geological maps (Altun *et al.*, 1990; Uğuz *et al.*, 2002), it is shown as “granite”. The Geme Complex consists mainly of gneiss and migmatite with minor amphibolite, marble and cross-cutting granitic veins and stocks. It is intruded by a

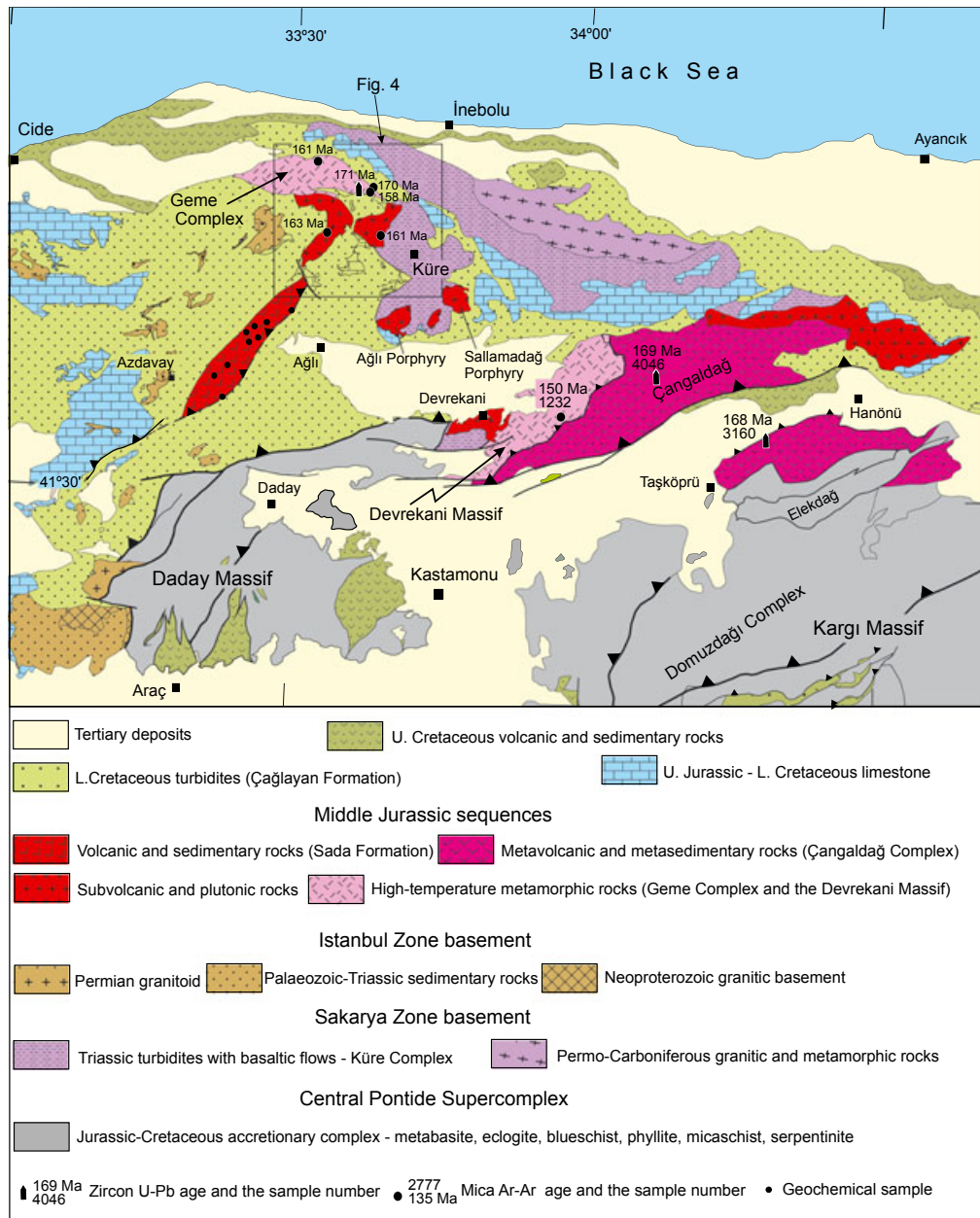


Fig. 3. Geological map of the northern Central Pontides.

porphyry body and is unconformably overlain by Lower Cretaceous sandstone and shale (Figs 3 & 4).

Medium-grained, banded, aluminous gneiss makes up more than 70% of the outcrops. The banding is defined by mm-scale intercalation of quartzofeldspathic layers with darker layers of biotite, cordierite and sillimanite (Fig. 5a). The characteristic mineral assemblage in the gneiss is quartz + K-feldspar + plagioclase + biotite + cordierite ± sillimanite ± garnet (Fig. 6). Migmatite is the next common rock type; it consists of various proportions of restite and the leucosome (Fig. 5b). Amphibolite makes <5% of the outcrops and forms medium- to coarse-grained

banded rocks with the common mineral assemblage hornblende + plagioclase + diopside. The banding is defined by the mm- to cm-thick intercalation of the hornblende- and diopside-rich layers. Granitic veins, ranging in thickness from a few centimetres to several metres, cross-cut the banding (Fig. 5d) and make up about 10% of the Gême Complex.

The prominent structure in the Gême Complex is a moderately to steeply dipping millimetre-scale compositional banding, which is distorted and convoluted in the migmatitic portions. A subvertical mylonitic foliation (Fig. 5c) and a weak subhorizontal mineral lineation are only observed in the metamorphic

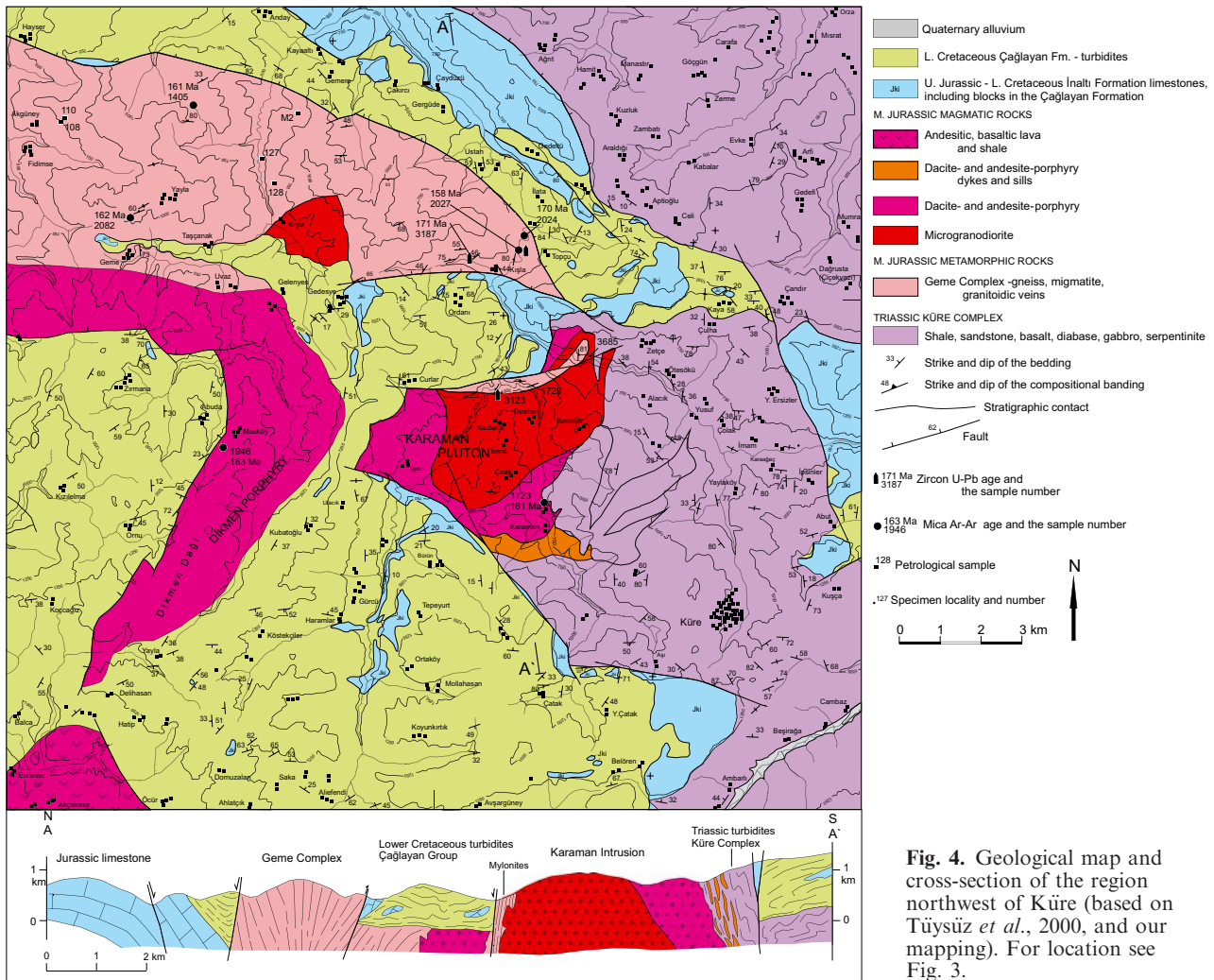


Fig. 4. Geological map and cross-section of the region northwest of Küre (based on Tüysüz *et al.*, 2000, and our mapping). For location see Fig. 3.

outlier north of the Karaman Pluton (Fig. 4). The mylonitic fabric is cut by the Karaman Pluton. This portion of the Geme Complex must have formed prior to 161 Ma, likely at a deep level of a strike-slip fault zone.

Mineral chemistry

Minerals from four gneiss samples and two amphibolites from the Geme metamorphic rocks were analysed by electron microprobe in the Ruhr-Universität Bochum. The estimated mineral assemblages of the analysed samples are shown in Table 1, and representative mineral compositions are given in Table 2. The analytical methods are described in Appendix S1.

Garnet in the gneiss forms poikilitic or skeletal porphyroblasts (Fig. 6a), making up <5% of the rock. The inclusions in garnet comprise all other minerals in the rock, including cordierite and biotite. Garnet is composed mainly of almandine (67–82%) with minor spessartine (8–20%), pyrope (5–15%) and grossular (2–5%) components (Fig. 7a). Garnet does not show

zoning with minor compositional variation within a single thin section (Fig. 7a). Cordierite generally makes up between 10 and 20% of the rock. It shows various degrees of pinitization. The Fe/(Fe+Mg) ratio in the fresh cordierite ranges between 0.4 and 0.6 with minor variation within a single sample (Fig. 7b). Sillimanite occurs in fibrolitic form and is spatially associated with biotite and cordierite (Fig. 6); it makes up between 2 and 4% of the rock. Biotite is found as reddish brown crystals in the gneiss making up between 10 and 30% of the rock. The Fe/(Fe+Mg) ratio in the analysed biotite ranges between 0.5 and 0.8 (Fig. 7b). Both plagioclase and K-feldspar are present in the gneiss comprising between 20 and 50% of the rock. The anorthite content of the plagioclase in the gneiss is highly variable and ranges between 1 and 35% (Fig. 7c). The compositional variation between grains in a single thin section is much greater than any zoning in a single grain. Plagioclase is more calcic in the amphibolite (20–90% anorthite) and makes up 35–45% of the rock. The large range in the anorthite content of the analysed plagioclase crystals is possibly due

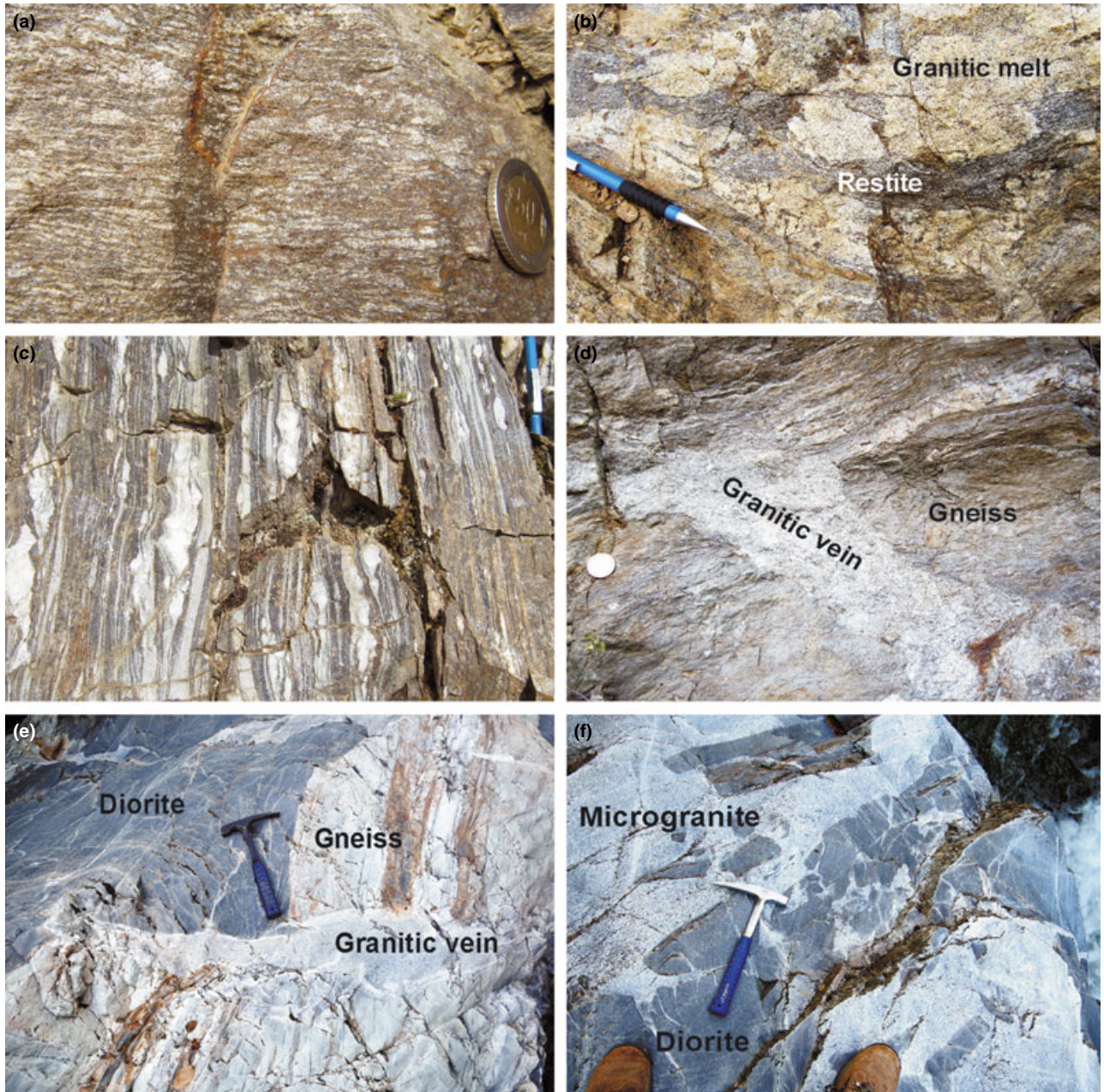


Fig. 5. Field photographs of the Geme Complex and the Karaman pluton (a) Banded gneiss, locality 2032. (b) Migmatite with banded biotite-rich restite and granitic melt, locality 2032. (c) Mylonitic gneiss, locality 1729. (d) Granitic vein in banded gneiss, locality 3186. (e) Diorite of the Karaman pluton cutting the gneiss of the Geme Complex. A late granitic vein cuts through the diorite and the gneiss, locality 3123. (f) Early diorite intruded and net-veined by microgranite, Karaman intrusion, locality 3123.

to late alteration leading to leaching of Ca; this is based on strong intra-grain compositional variation between the plagioclase grains, and the prevalent pinization of cordierite suggesting late-stage fluid influx. K-feldspar is close to the end-member composition with minor Na and Ca (Table 2). Diopside occurs as pale green granular crystals in the amphibolite comprising 30 to 40% of the rock. The Fe/(Fe+Mg) ratio of the diopside ranges between 0.32 and 0.65 (Fig. 7b). Hornblende forms brown to dark green crystals of

tschermakite and hornblende composition. Accessory minerals include ilmenite in gneiss and amphibolite, and titanite and epidote in the amphibolite.

P–T conditions of metamorphism

The peak *P–T* conditions of the metamorphism in the Geme Complex were estimated using the mineral assemblages and mineral compositions from the analysed rocks. Activities were determined from mineral

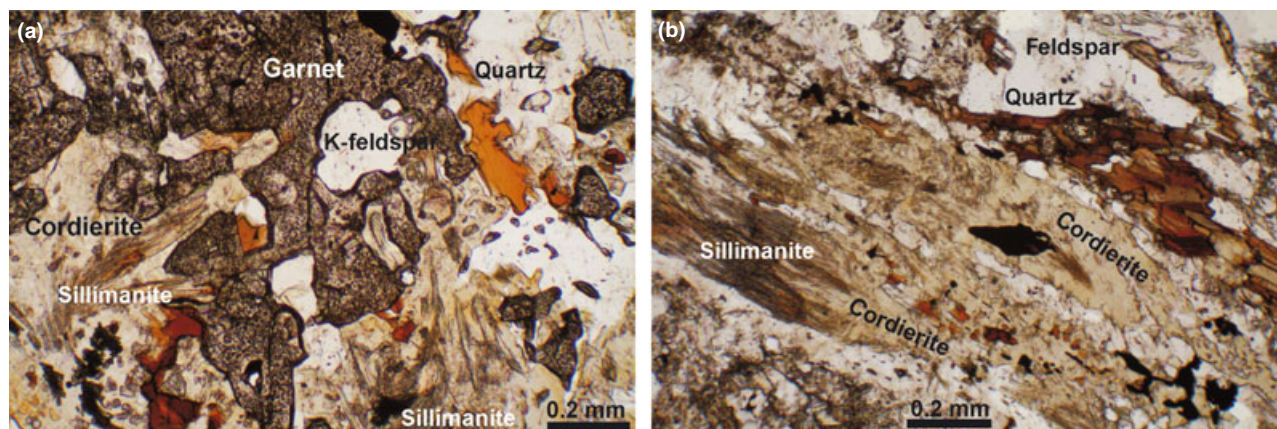


Fig. 6. Photomicrographs from the Geme Complex. (a) Gneiss with garnet, sillimanite, pinitized cordierite, biotite (reddish brown), quartz and K-feldspar, sample 127-3. (b) Gneiss with sillimanite, pinitized cordierite, biotite (reddish brown), quartz, feldspar and opaque, sample 127-4.

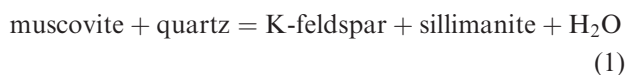
Table 1. Estimated modal amounts in the analysed samples from the Geme Complex.

| Sample no. | Gneiss | | | | Amphibolite | |
|------------|--------|-------|-----|----|-------------|-------|
| | 127-3 | 127-4 | 128 | M2 | 108 | 110-3 |
| Crđ | 13 | 15 | – | 18 | – | – |
| Grt | 1 | 2 | 2 | 3 | – | – |
| Sil | 4 | 2 | – | – | – | – |
| Bt | 22 | 25 | 8 | 28 | – | – |
| Pl | 36 | 31 | 48 | 22 | 37 | 41 |
| Kfs | – | – | – | – | – | – |
| Qz | 21 | 23 | 40 | 27 | – | – |
| Di | – | – | – | – | 33 | 35 |
| Hbl | – | – | – | – | 24 | 20 |
| Ilm | 2 | 2 | tr | 2 | 2 | – |
| Mag | 1 | – | – | – | – | 2 |
| Ep | – | – | – | – | 2 | – |
| Ttn | – | – | – | – | 2 | 1 |
| Chl | – | – | 2 | tr | tr | 1 |
| Ap | – | tr | tr | tr | – | – |

tr, < 0.5%.

compositions using the AX program (<http://www.ccp14.ac.uk/ccp/web-mirrors/crush/astaff/holland/ax.html>) at 720° C and 4 kbar.

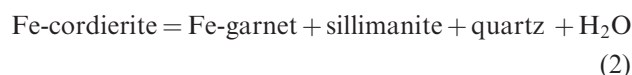
The general absence of muscovite and presence of sillimanite + K-feldspar indicate that the peak temperatures were above 700° C, based on the reaction (1):



Garnet-biotite geothermometry, based on the thermodynamic data set of Holland & Powell (1998) and the THERMOCALC program of Powell & Holland (1988), indicates temperatures only in the range of 600 and 675° C for 4 kbar (Fig. 8), probably due to the retrograde readjustment of the biotite and garnet compositions.

The absence of muscovite and presence of sillimanite constrain the metamorphic pressures between 1 and 9 kbar (Fig. 8). The presence of cordierite indicates that the pressures were in the lower part of this

range. Fe-cordierite reacts to garnet and sillimanite at 3.5–4.0 kbar through the reaction (2) (Fig. 8):



The coexistence of cordierite, garnet, sillimanite and quartz in the gneiss of the Geme Complex (Fig. 6) indicates that the peak *P–T* conditions were close to reaction (2). Pressure estimates using representative compositions from sample 127-3 (Table 2), the thermodynamic data set of Holland & Powell (1998) and the THERMOCALC program of Powell & Holland (1988) with activities determined using the AX program (<http://www.ccp14.ac.uk/ccp/web-mirrors/crush/astaff/holland/ax.html>) indicate a pressure of ~4 kbar at a given temperature of 720° C. Mineral assemblages and mineral compositions indicate that the peak *P–T* conditions during the metamorphism of the Geme Complex were 4 ± 1 kbar and 720 ± 40 °C (Fig. 8).

Geochronology

There is no previous isotopic data on the age of metamorphism of the Geme Complex. This Complex is intruded by the Middle Jurassic (163 Ma) Dikmen Porphyry providing a pre-Callovian metamorphic age. Stratigraphic relations show that the Geme Complex was on the surface by the Early Cretaceous (Barremian-Aptian). Zircon and biotite from the Geme Complex were dated, using laser ablation IC-PMS U–Pb technique in UC Santa Barbara, and the Ar–Ar single-grain fusion method in the Open University, UK, respectively, to determine the timing of its metamorphic history. The locations of the dated samples are shown in Fig. 4, and the age data are summarized in Table 3. The Ar–Ar and the U–Pb analytical data are given in Tables S1 and S2, respectively. Methods of the mineral separation and dating

Table 2. Representative mineral compositions from the Geme Complex.

| | Cordierite gneiss – 127-3 | | | | | | | Cordierite gneiss – M2 | | | | Amphibolite – 108 | | | |
|--------------------------------|---------------------------|--------|-------|--------|--------|-------|--------|------------------------|-------|-------|--------|-------------------|--------|-------|--|
| | Crld | Grt | Bt | Pl | Kfs | Sill | Ilm | Crld | Grt | Bt | Pl | Pl | Cpx | Hbl | |
| | 8 | | 22 | 12 | 16 | 5 | 19 | 62 | 41 | 42 | 55 | 219 | 239 | 233 | |
| SiO ₂ | 47.86 | 36.59 | 33.77 | 61.71 | 66.55 | 37.25 | 0.03 | 48.69 | 37.11 | 35.34 | 64.50 | 56.60 | 51.79 | 41.84 | |
| TiO ₂ | 0.00 | 0.02 | 5.04 | 0.01 | 0.02 | 0.00 | 52.78 | 0.02 | 0.04 | 3.93 | 0.01 | 0.03 | 0.03 | 2.44 | |
| Al ₂ O ₃ | 32.26 | 20.25 | 17.46 | 25.44 | 18.36 | 61.66 | 0.02 | 31.77 | 20.61 | 17.89 | 22.77 | 26.85 | 0.63 | 10.45 | |
| Cr ₂ O ₃ | 0.02 | 0.01 | 0.17 | 0.00 | 0.00 | 0.09 | 0.22 | 0.05 | 0.10 | 0.24 | 0.00 | 0.00 | 0.01 | 0.02 | |
| FeO | 13.43 | 36.25 | 23.56 | 0.07 | 0.03 | 0.20 | 46.69 | 9.45 | 30.43 | 18.92 | 0.16 | 0.29 | 14.73 | 20.66 | |
| MnO | 0.18 | 4.39 | 0.09 | 0.04 | 0.00 | 0.03 | 0.50 | 0.57 | 7.44 | 0.28 | 0.01 | 0.02 | 0.35 | 0.28 | |
| MgO | 5.32 | 1.62 | 5.64 | 0.00 | 0.01 | 0.03 | 0.14 | 7.29 | 3.27 | 9.27 | 0.00 | 0.00 | 9.42 | 8.14 | |
| CaO | 0.06 | 1.11 | 0.02 | 6.37 | 0.06 | 0.03 | 0.01 | 0.00 | 0.91 | 0.01 | 4.65 | 10.01 | 23.00 | 11.03 | |
| Na ₂ O | 0.11 | 0.03 | 0.08 | 7.59 | 1.31 | 0.01 | 0.00 | 0.25 | 0.03 | 0.15 | 8.74 | 5.84 | 0.12 | 2.36 | |
| K ₂ O | 0.01 | 0.06 | 9.37 | 0.10 | 15.14 | 0.00 | 0.01 | 0.00 | 0.00 | 9.33 | 0.13 | 0.15 | 0.01 | 0.49 | |
| total | 99.25 | 100.33 | 95.20 | 101.33 | 101.48 | 99.30 | 100.40 | 98.09 | 99.94 | 95.36 | 100.97 | 99.79 | 100.09 | 97.71 | |
| Cations on the basis of | | | | | | | | | | | | | | | |
| | 18 O | 12 O | 11 O | 8 O | 8 O | 5 O | 3 O | 18 O | 12 O | 11 O | 6 O | 8 O | 6 O | 23 O | |
| Si | 5.00 | 2.99 | 2.64 | 2.70 | 3.01 | 1.01 | 0.00 | 5.06 | 3.00 | 2.69 | 2.82 | 2.55 | 1.99 | 6.42 | |
| Ti | 0.00 | 0.00 | 0.30 | 0.00 | 0.00 | 0.00 | 1.00 | 0.00 | 0.00 | 0.23 | 0.00 | 0.00 | 0.00 | 0.28 | |
| Al | 3.97 | 1.95 | 1.61 | 1.31 | 0.98 | 1.98 | 0.00 | 3.89 | 1.96 | 1.61 | 1.17 | 1.43 | 0.03 | 1.89 | |
| Cr | 0.00 | 0.00 | 0.01 | 0.00 | 0.00 | 0.00 | 0.00 | 0.00 | 0.01 | 0.01 | 0.00 | 0.00 | 0.00 | 0.00 | |
| Fe | 1.17 | 2.48 | 1.54 | 0.00 | 0.00 | 0.00 | 0.98 | 0.82 | 2.06 | 1.20 | 0.01 | 0.01 | 0.47 | 2.65 | |
| Mn | 0.02 | 0.30 | 0.01 | 0.00 | 0.00 | 0.00 | 0.01 | 0.05 | 0.51 | 0.02 | 0.00 | 0.00 | 0.01 | 0.04 | |
| Mg | 0.83 | 0.20 | 0.66 | 0.00 | 0.00 | 0.00 | 0.01 | 1.13 | 0.39 | 1.05 | 0.00 | 0.00 | 0.54 | 1.86 | |
| Ca | 0.01 | 0.10 | 0.00 | 0.30 | 0.00 | 0.00 | 0.00 | 0.00 | 0.08 | 0.00 | 0.22 | 0.48 | 0.95 | 1.81 | |
| Na | 0.02 | 0.00 | 0.01 | 0.64 | 0.12 | 0.00 | 0.00 | 0.05 | 0.00 | 0.02 | 0.74 | 0.51 | 0.01 | 0.70 | |
| K | 0.00 | 0.00 | 0.94 | 0.01 | 0.87 | 0.00 | 0.00 | 0.00 | 0.00 | 0.91 | 0.01 | 0.01 | 0.00 | 0.10 | |
| total | 11.02 | 8.03 | 7.72 | 4.97 | 4.99 | 3.00 | 2.00 | 11.01 | 8.02 | 7.74 | 4.97 | 4.99 | 4.00 | 15.75 | |

O, oxygen.

are described in Appendix S1 and the petrography of the dated samples in S2.

Zircon was dated from one gneiss sample (sample 2024) and from a 1 m thick granitic vein (3187) cross-cutting the gneissic banding. The gneiss sample has only inherited zircon with ages ranging from 378 to 2850 Ma (T. Zack pers. comm.), suggesting a sedimentary origin for the gneiss. Zircon from the granitic vein, on the other hand, shows two distinct age populations; seven of 25 zircon grains dated, form a tight age cluster at 172 ± 3 Ma (Fig. 9a); this zircon is euhedral and shows distinct oscillatory zoning typical for magmatic zircon (Fig. 10), and is interpreted to have crystallized from melt. The widespread evidence for partial melting in the metamorphic rocks indicates that the granitic melt was formed during the high-temperature metamorphism, as also suggested by abundant inherited zircon in the granitic vein and in the granitic intrusions. Therefore, the peak metamorphism must have been very close to 172 Ma.

Biotite was dated using single-grain fusion of individual grains from three gneiss samples and from a granitic vein. The granitic sample 2027 comes from a 10 m thick vein, which cross-cuts the banding in the surrounding gneiss. Biotite from the granitic vein gave an Ar–Ar biotite age of 158 ± 5 Ma (Fig. 11). The biotite Ar–Ar ages from the three gneiss samples (1405, 2024 & 2082) are *c.* 164 Ma (Table 3; Fig. 11). Thus, the isotopic data indicate that the peak metamorphic temperatures during the metamorphism of the Geme Complex were reached at *c.* 172 Ma, and the rocks cooled to 300 °C, the generally accepted closure age for Ar–Ar in biotite (e.g. Harrison *et al.*, 1985), at *c.* 164 Ma, when they were intruded by granitic bodies.

The inherited zircon grains in the Geme Complex and in the granitoids provide an indication of the source region. They are predominantly late Neoproterozoic and Palaeozoic with few Palaeoproterozoic and late Archean zircon (Fig. 12). The Archean zircon is rounded (Fig. 10) and is probably derived from the East European Craton, whereas the late Neoproterozoic zircon is euhedral with igneous zoning. Some of the late Neoproterozoic zircon grains have Carboniferous rims (Fig. 10). The Pontides are characterized by a late Neoproterozoic and Hercynian basement, and the dominance of zircon of these ages in the Geme Complex suggests that the Geme Complex represents the remobilized basement of the Central Pontides.

The Devrekani Massif

The Devrekani Massif is a NE–SW-oriented metamorphic body in the southern part of the Central Pontides, 27 km long and 6 km wide (Fig. 3). It consists of gneiss, marble and amphibolite, and is intruded by the Middle Jurassic Devrekani granitoid (Yılmaz, 1980, 1981). Lower Cretaceous turbidites lie unconformably over the Devrekani metamorphic rocks. The critical mineral assemblage in the gneiss is quartz + K-feldspar + plagioclase + biotite ± muscovite ± sillimanite ± garnet (Yılmaz, 1981). The widespread presence of muscovite indicates that the peak metamorphic temperatures must have been less than that of the Geme Complex.

One gneiss sample (1232) from the Devrekani Massif was dated to constrain the age of metamorphism (Fig. 3). The gneiss consists of quartz + plagioclase

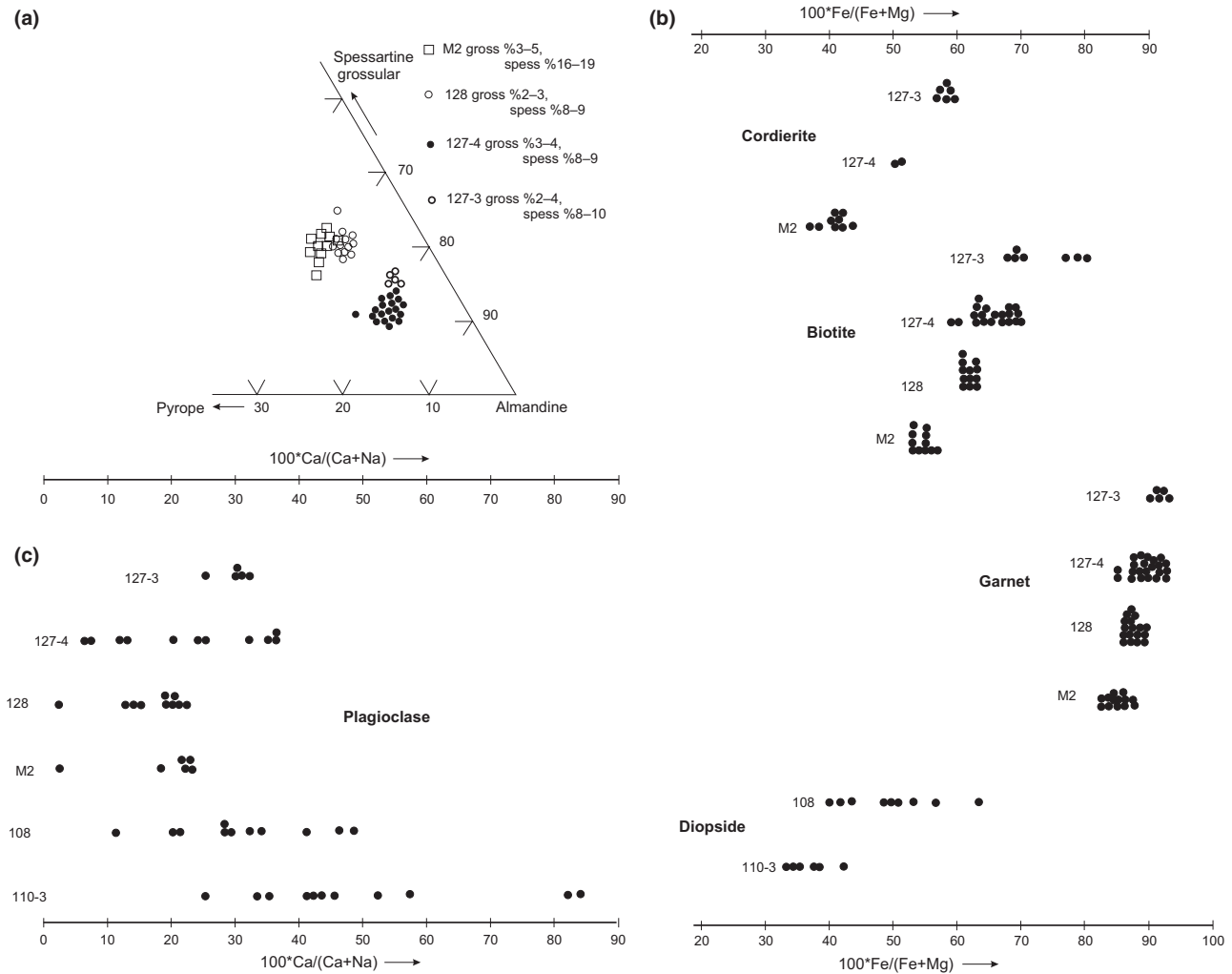


Fig. 7. Mineral compositions from the gneiss and amphibolite of the Geme Complex. (a) Garnet compositions plotted on the almandine – pyrope – grossular + spessartine ternary diagram. (b) Fe/(Fe+Mg) ratios in cordierite, biotite, garnet and diopside. (c) Anorthite contents of the plagioclase.

class + K-feldspar + muscovite + biotite. The muscovite and biotite cooling ages from this sample are 151 and 146 Ma, respectively (Table 3). The Devrekani metamorphic rocks are intruded by the Devrekani granitoid, which has well-constrained Middle Jurassic zircon U–Pb ages (*c.* 171 Ma, Nzegge, 2007). This suggests that the peak metamorphism in the Devrekani Massif is also likely to be Middle Jurassic.

MIDDLE JURASSIC MAGMATISM IN THE CENTRAL PONTIDES

The Jurassic magmatism in the Central Pontides comprises a number of shallow-level intrusions, lavas and volcanoclastic rocks. The compositions of the Jurassic volcanic rocks range from basic to acidic with a dominance of intermediate compositions (Boztuğ *et al.*, 1995). Here, we provide new petrographical, geochronological and geochemical data to determine the origin of the magmatism.

Shallow-level intrusions

In the Central Pontides, the granitic intrusions extend from close to the Black Sea coast 50 km southeast to the Devrekani region (Fig. 3). A Jurassic age for these plutons was first proposed by Yılmaz & Boztuğ (1986) and elaborated by Boztuğ *et al.* (1995). The age was based on the stratigraphic position of some of the intrusions, which cut the Upper Triassic Küre Complex and are unconformably overlain by the Upper Jurassic limestones (Fig. 2). Below, we briefly describe some of these intrusions for which new data are provided.

Dikmen Porphyry

This is a shallow-level intrusion made up of monotonous, strongly porphyritic grey andesite to dacite. It intrudes the Geme metamorphic complex in the north and is unconformably overlain by the Lower Creta-

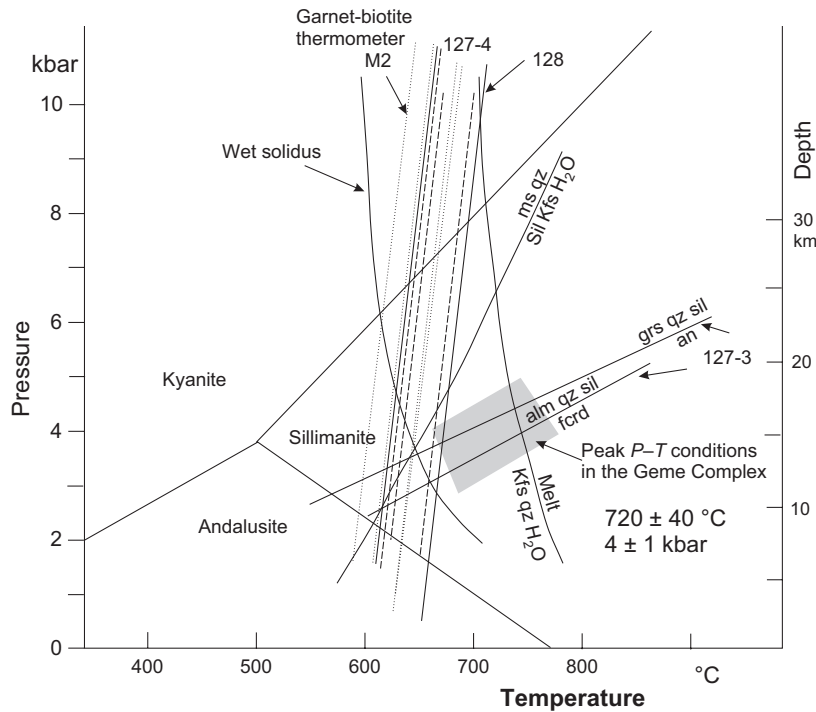


Fig. 8. Pressure–temperature diagram showing the conditions of metamorphism of the Geme Complex. The reactions are calculated using the THERMOCALC program of Powell & Holland (1988).

Table 3. New geochronological ages from the Jurassic metamorphic and magmatic rocks.

| Unit | Rock type | Sample No. | Location (UTM Coordinates) | Ar–Ar biotite ages (Ma) | U–Pb zircon ages (Ma) | |
|-------------------|---------------|------------|----------------------------|-------------------------|-----------------------|---------------|
| | | | | | Age range | Young cluster |
| Geme Complex | Gneiss | 1405 | 36T 05 46 000–46 40 894 | 161 ± 3 | – | – |
| | Gneiss | 2024 | 36T 05 54 178–46 37 785 | 169 ± 5 | – | – |
| | Gneiss | 2082 | 36T 05 44 491–46 38 116 | 162 ± 11 | – | – |
| | Granitic vein | 2027 | 36T 05 53 893–46 37 383 | 158 ± 5 | – | – |
| | granitic vein | 3187 | 36T 05 52 802–46 37 283 | – | 168–835 | 172 ± 2 |
| Devrekani Massif | Gneiss | 1232 | 36T 05 79 979–46 05 196 | 146 ± 2 | – | – |
| | Gneiss | 1232 | 36T 05 79 979–46 05 196 | 151 ± 1 (mu) | – | – |
| Dikmen Porphyry | Dacite | 1946 | 36T 05 46 820–46 32 484 | 163 ± 4 | – | – |
| | Dacite | 1723 | 36T 05 54 646–46 31 215 | 162 ± 4 | – | – |
| Karaman Pluton | Granodiorite | 3123 | 36T 05 53 340–46 33 974 | – | 389–2779 | – |
| | Metadacite | 3160 | 36T 06 10 032–46 04 333 | – | – | 168 ± 1 |
| Çangaldağ Complex | Metadacite | 4046 | 36T 05 92 750–46 12 765 | – | – | 169 ± 2 |

The UTM coordinates are in European 1979 grid, which is closely compatible with the 1:25 000 scale topographic maps of Turkey. For full analytical data see Table S1 in the supplementary data. mu, muscovite age.

ceous turbidites (Fig. 4). The Dikmen porphyry is made up of biotite, zoned plagioclase and rare quartz and very rare hornblende phenocrysts, about 0.5 mm in size, set in a fine-grained matrix consisting of the same minerals (Appendix S2). The intrusion is coarser grained along its eastern margin. It shows a strong late-stage alteration involving replacement of biotite by chlorite.

There are no published age data on the Dikmen Porphyry. Ten biotite grains from one dacite–porphyry sample (1946) were dated by Ar–Ar laser probe technique; the biotite gives a coherent age of 163 Ma (Table 3; Fig. 11). Considering the porphyritic nature of the rock and the strongly zoned plagioclase phenocrysts, and lack of a contact metamorphic aureole, all

indicative of a shallow intrusion level, the Ar–Ar data indicate a Middle Jurassic (Callovian) crystallization age for the Dikmen Porphyry.

Karaman Pluton

The Karaman Pluton, located northwest of Küre, forms an irregular body measuring 5 km by 5 km (Fig. 4). It intrudes the Triassic Küre Complex and a small outlier of Geme metamorphic rocks in the northwest and is unconformably overlain by the Lower Cretaceous turbidites (Boztuğ, 1992; Boztuğ *et al.*, 1995). The Karaman intrusion shows a zonal structure with a core of medium-grained microgranodiorite to microdiorite surrounded by dacite–

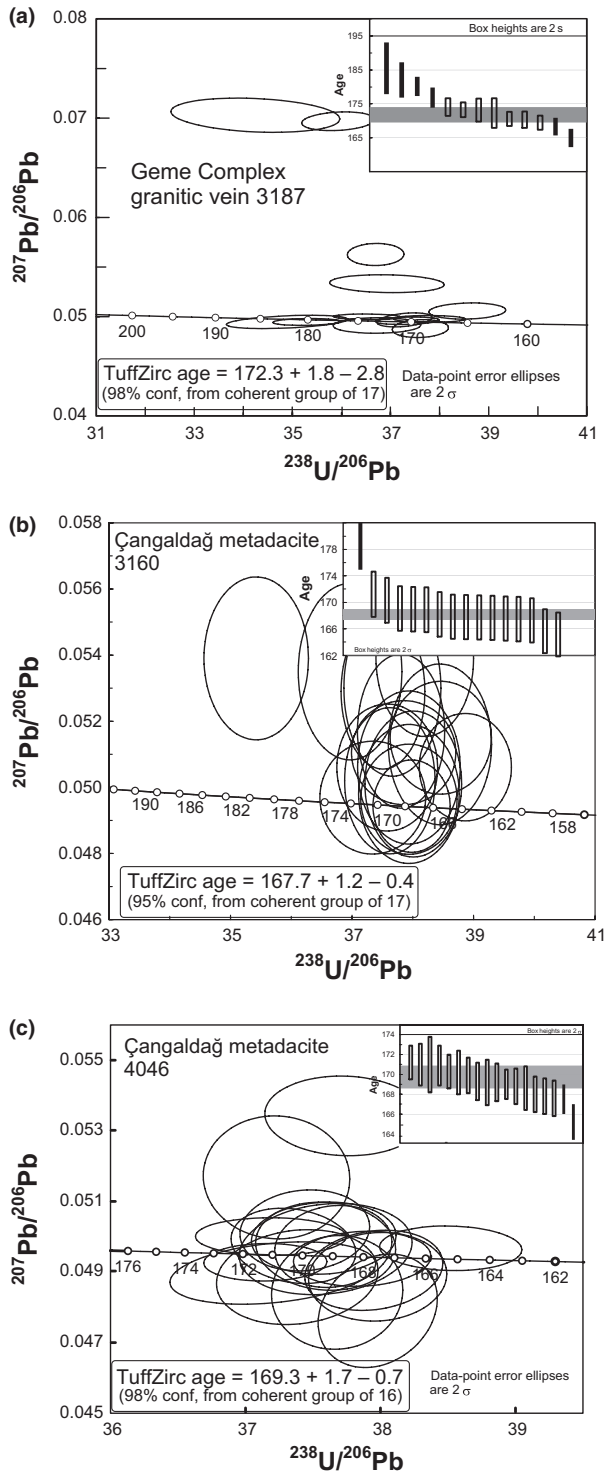


Fig. 9. Zircon U–Pb diagrams from the Geme Complex and the Karaman intrusion.

porphyry. In the west, it is probably connected to the Dikmen intrusion under the Cretaceous cover (Fig. 4).

The earliest intrusion was a diorite of plagioclase + biotite + hornblende, and is cut by volumi-

nous microgranodiorite (Fig. 5e,f). At one locality (3865 in Fig. 4), there is also a 10 m large gabbro-peridotite body in the granodiorite, probably representing a relict cumulate from the initial mafic magma. The mineral assemblage in the microgranodiorite, which makes the bulk of the intrusion, is plagioclase + biotite + quartz ± hornblende ± cordierite. The marginal dacite–porphyry consists of plagioclase, biotite, quartz and locally hornblende phenocrysts in a fine-grained matrix of the same minerals. Other rare phenocryst phases include garnet and augite. As in the Dikmen Porphyry, the biotite in the Karaman intrusion is partially to totally replaced by chlorite.

Biotite and zircon have been dated from two samples from the Karaman intrusion to constrain its age. There are no previous published age data on the intrusion. The zircon ages from the microgranodiorite (sample 3123) show a wide scatter from 2819 to 377 Ma (Fig. 12), indicating that the zircon is inherited. On the other hand, 10 biotite grains from a dacite–porphyry sample (1723) gave a coherent age of 162 Ma (Table 3; Fig. 11), similar to those from the Dikmen Porphyry (*c.* 163 Ma).

Ağlı, Sallamadağ and Devrekani intrusions

The Ağlı Porphyry cuts the Upper Triassic Küre Complex and is unconformably overlain by the Upper Jurassic limestones (Fig. 3). It was the first intrusion in the Central Pontides whose Jurassic age was established by the regional stratigraphy (Yılmaz & Boztuğ, 1986). Aydın *et al.* (1995) mentioned a Late Jurassic (154 ± 2 Ma) Rb–Sr age from the Ağlı Porphyry. The Sallamadağ intrusion to the east of the Ağlı porphyry also intrudes the Triassic Küre Complex. Petrographically, the Ağlı and Sallamadağ intrusions are similar to the Dikmen Porphyry, and consists of zoned plagioclase, biotite, quartz and rare hornblende phenocrysts in a fine-grained matrix of the same minerals. Biotite is again extensively chloritized. The Devrekani intrusion is a large pluton northeast of Kastamonu. It intrudes the Devrekani metamorphic rocks and is unconformably overlain by the Lower Cretaceous turbidites. It is a metaluminous, tholeiitic to calcalkaline diorite to tonalite with a porphyritic texture and consists of plagioclase, biotite, hornblende and quartz (Nzegge, 2007). Zircon from four diorite samples produced Middle Jurassic U–Pb ages ranging from 170 to 165 Ma (Nzegge, 2007).

Jurassic volcanic, volcanoclastic and clastic series

The Middle Jurassic volcanic and volcanoclastic rocks in the Central Pontides include the Sada Formation in the north and the Çangaldağ Complex in the south. Basaltic to andesitic lavas, breccias, interca-

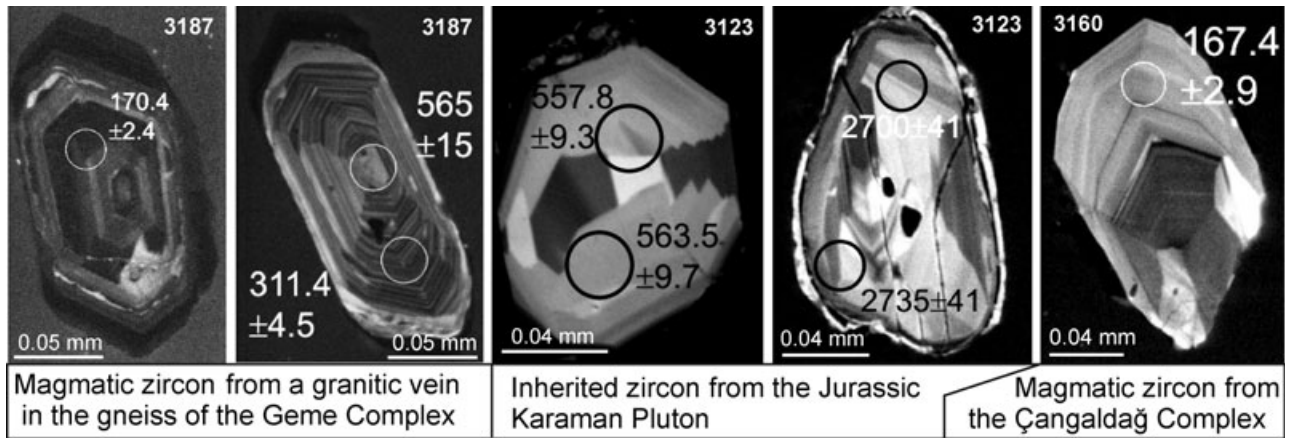


Fig. 10. Cathodoluminescence images of zircon from the Central Pontides that are dated using laser ablation ICP-MS. The laser ablation pits, marked by circles, are 25 μm in diameter.

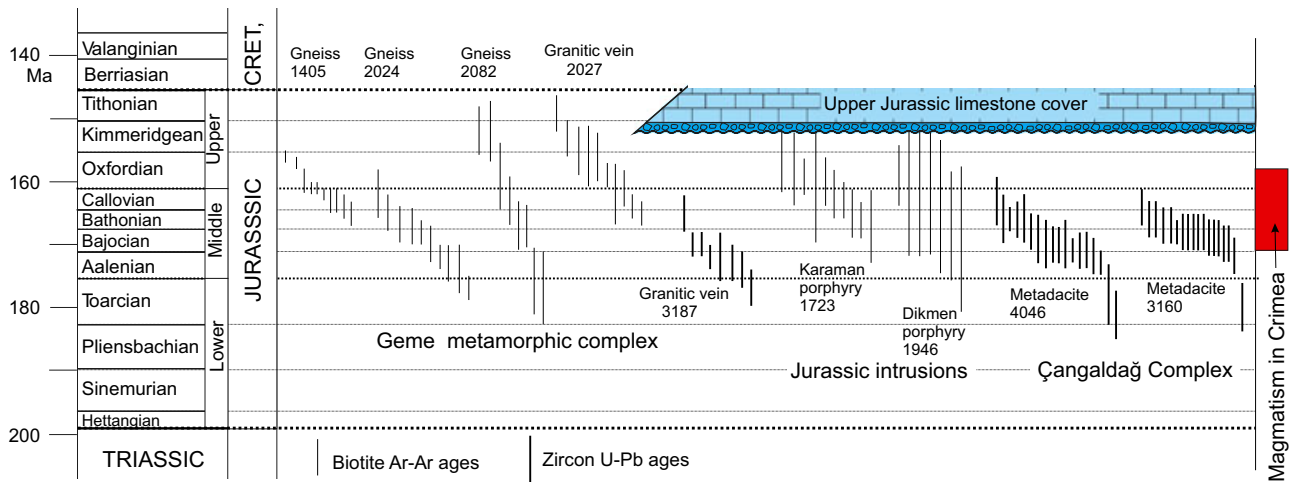


Fig. 11. New isotopic ages from the metamorphic and magmatic rocks of the Central Pontides. Each vertical bar represents a single biotite or zircon age. The age range of the magmatism in Crimea is from Meijers *et al.* (2010).

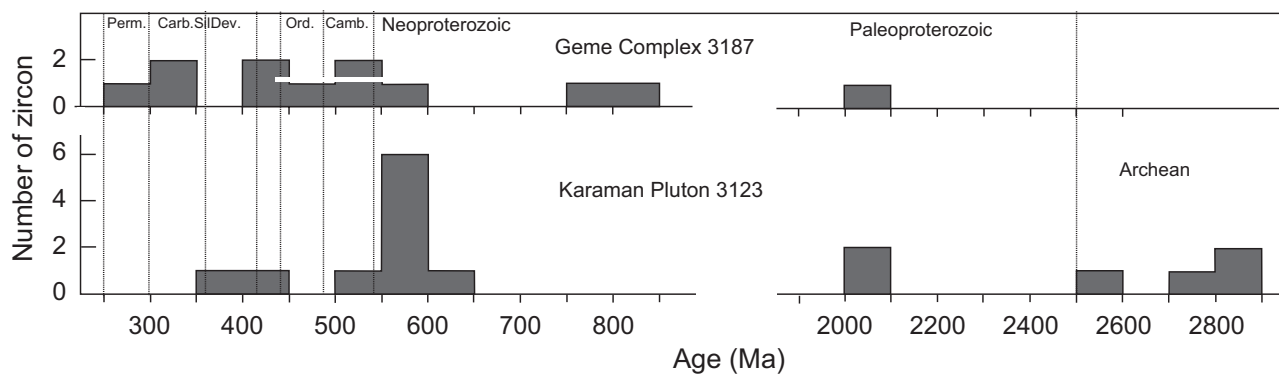


Fig. 12. Age histogram of the inherited zircon from the Geme Complex and the Karaman Pluton.

lated with dark shales, mudstones and siltstones, called the Sada Formation (Tüysüz *et al.*, 2000), crop out southwest of the Dikmen Porphyry at the base of

a thrust sheet (Fig. 3). Radiolaria from the intercalated mudstones indicate a Callovian to Oxfordian age (Bragin *et al.*, 2002).

The Çangaldağ Complex is an over 10 km thick tectonic stack of volcanic, volcanoclastic and fine-grained clastic rocks metamorphosed in low-greenschist facies during the Early Cretaceous (Yılmaz, 1988; Ustaömer & Robertson, 1993; Okay *et al.*, 2013). It is interpreted either as a pre-Jurassic ophiolite (Yılmaz, 1988; Tüysüz, 1990) or as a pre-Jurassic ensimatic volcanic arc (Ustaömer & Robertson, 1993, 1994). The geochemistry of the volcanic rocks suggests the latter alternative (Ustaömer & Robertson, 1999). The volcanic rocks are mainly andesite with lesser amounts of basaltic andesite and dacite.

There are no geochronological data from the Çangaldağ Complex, which is generally regarded as Palaeozoic–Triassic in age (e.g. Ustaömer & Robertson, 1994). Zircon from two dacite–porphyries has been dated. Both gave similar ages of 168 and 169 Ma (Figs 9 & 11), which indicates that the magmatism is of Middle Jurassic age.

Geochemistry

New major oxide and trace element whole rock analyses are provided from 11 lava samples from the Sada Formation and seven samples from the Dikmen Porphyry to evaluate the origin of the Middle Jurassic magmatism. The analytical conditions are described in Appendix S1, and the geochemical data are given in Table S3.

The samples from the Sada lavas are generally strongly altered, and the loss on ignition (LOI) values range from 1.30 to 9.80%, suggesting variable hydrated nature (Table S3). High-field strength elements (Ti, Zr, Y, Nb & Hf), Th and REEs are used for classification and genetic considerations because they are regarded as immobile during low-grade metamorphism and alteration (e.g. Rollinson, 1993).

In general, the Sada lavas and Dikmen Porphyry display a wide-compositional range in their SiO₂ con-

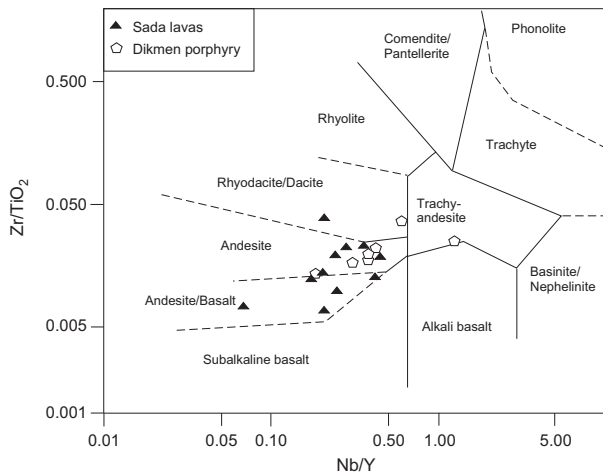


Fig. 13. Classification of the Sada lavas (filled triangles) and Dikmen Porphyry (hexagons) on the Zr/TiO₂ v. Nb/Y diagram (Winchester & Floyd, 1977).

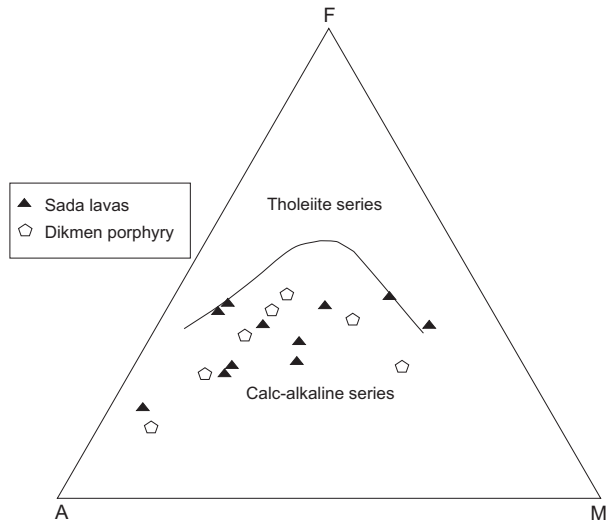


Fig. 14. Samples from the Sada lavas (filled triangles) and Dikmen Porphyry (hexagons) plotted on the AFM diagram of Irvine & Barager (1971) and showing a calcalkaline trend.

tents, recalculated on anhydrous basis, between 49.3–74.6 and 54.7–70.9 wt%, respectively. The Sada lavas are classified as subalkaline basalt, andesite and dacite on the Zr/TiO₂ v. Nb/Y plot of Winchester & Floyd (1977) (Fig. 13). Samples from the Dikmen Porphyry, on the other hand, classify as granodiorite and monzogranite on the Streckeisen (1976) classification diagram. On the basis of Nb/Y and Zr/TiO₂ ratios both the Sada lavas and the Dikmen Porphyry are (with the exception of one sample) subalkaline and intermediate according to the classification of Pearce (1996). On the AFM diagram, both the Sada lavas and the Dikmen Porphyry fall into the calcalkaline field (Fig. 14).

Chondrite normalized REE spidergrams of the Sada lavas and the Dikmen Porphyry show moderate enrichment in LREE with respect to HREE and slight to moderate negative Eu anomalies (Fig. 15a). The La_n/Yb_n values are mostly in the range of 2.3–6.8 for the Sada lavas, and 6.0–13.1 for the more acidic Dikmen Porphyry; there is gradation in the La_n/Yb_n values, rather than a gap between two magmatic suites suggesting a common magmatic source. The negative Eu anomalies (Eu_n/(Sm_n*Gd_n)^{0.5}) are in the range of 0.72–0.95 for the Sada lavas (with the exception of one sample with 1.1) and 0.61–0.77 for the Dikmen Porphyry. All these geochemical features suggest fractionation of plagioclase during the magma chamber evolution of these two magmatic series. Absence of a marked depletion in HREEs with respect to the MREEs and LREEs rules out involvement of significant amount of garnet in the generation and fractionation of these magmas.

In N-MORB-normalized spider diagrams, there are selective enrichments in fluid-mobile LILE (Large Ion Lithophile Elements: Sr, K, Rb, Ba & Th) and, to a lesser extent, in LREEs (La to Nd) and deple-

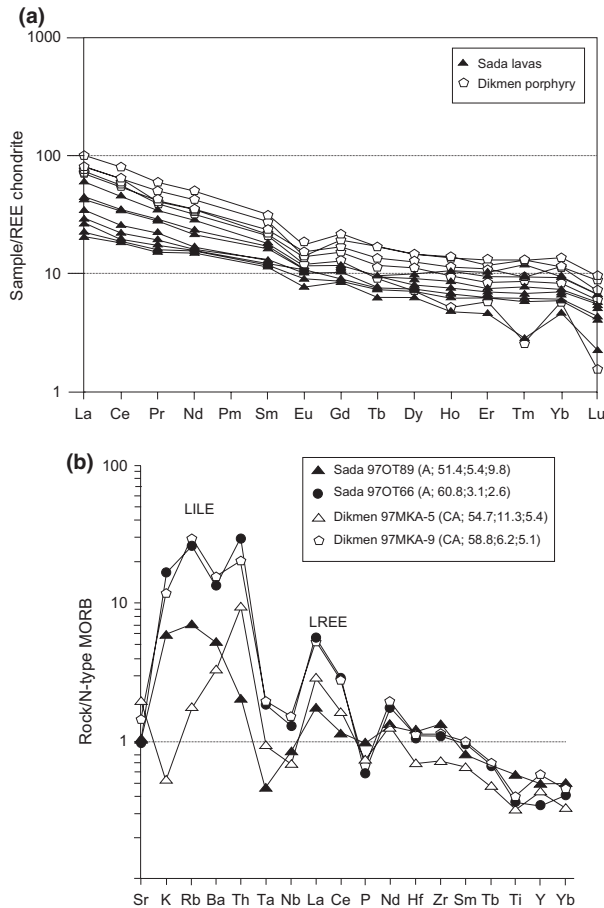


Fig. 15. (a). Chondrite-normalized rare earth element abundance patterns normalized to values given in Boynton (1984). (b) N-type MORB normalized multi-element spidergrams of the Sada lavas and Dikmen Porphyry. The elements are arranged in the order suggested by Pearce (1983). Normalization values are those of Sun & McDonough (1989). The numbers given in parentheses in the legend are percentages of silica, MgO and LOI respectively.

tion in fluid immobile HFS (High-Field Strength) elements (e.g. Ta, Nb & Zr) (Fig. 15b). All samples exhibit negative anomalies of Ta and Nb relative to their adjacent LILE and LREE. These geochemical features are characteristic for arc-related magmas (e.g. Pearce & Peate, 1995).

The selective enrichment of LILEs and LREEs relative to HFSEs is consistent with their derivation from a mantle source enriched by a subduction component. Although the assimilation of the continental crust may create a similar effect on MORB-normalized patterns by resulting a depletion in Nb and Ta and, to a lesser extent, in Hf and Zr, it could not be responsible for these patterns because even the most primitive lavas display the above mentioned subduction component.

In a Ta/Yb v. Th/Yb plot, on which only the basic to intermediate (i.e. $\text{SiO}_2 < 60\%$) lavas are plotted together with the well-established mantle composi-

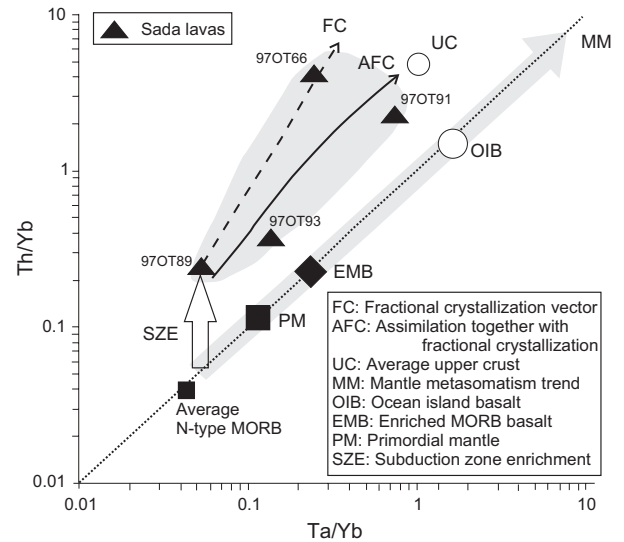


Fig. 16. Th/Yb v. Ta/Yb diagram (after Pearce, 1983) for basaltic and basaltic andesitic Sada lavas (i.e. the ones with $\text{SiO}_2 < 60$ wt.%). The upper crustal composition is after Taylor & McLennan (1985).

tions such as OIB, EMB, PM and NMB (explanations are in Fig. 16) and the average composition of upper crust (Taylor & McLennan, 1985), the Sada lavas exhibit a consistent displacement from the mantle metasomatism array (MM) towards higher Th/Yb values, forming a trend sub-parallel to the MM array (Fig. 16). Note that the fractional crystallization vector (i.e. FC) and the AFC curve starting from the possible basaltic end-member composition (i.e. sample 97 OT 89) are also plotted for comparison. This observation also suggests that these lavas were derived from a depleted mantle source (i.e. similar to the N-type MORB) containing a distinct subduction component and evolved via fractional crystallization (e.g. 97-OT66) and AFC (e.g. 97-OT93 & 97-OT91) processes.

Samples of the Dikmen Porphyry and intermediate to acid lavas of Sada formation fall into the volcanic-arc field on the Pearce *et al.* (1984) diagrams. To sum up, the geochemistry of the Sada lavas and the Dikmen Porphyry suggests formation in a volcanic arc.

JURASSIC MAGMATISM IN THE PONTIDES, CAUCASUS AND IRAN

Below, we review the Jurassic magmatism farther east to establish a regional frame for magmatism, sedimentation and tectonic setting.

Jurassic volcanic, volcanoclastic and clastic series in the Pontides

Lower–Middle Jurassic volcanoclastic and volcanic sequences, known as the Kelkit Formation, are wide-

spread in the Eastern Pontides and constitute the lateral equivalent of the Sada Formation (Fig. 1). The Kelkit Formation consists of shallow marine volcanoclastic, clastic and volcanic sequences with rare Ammonitico Rosso type limestone and marl horizons (Bergougnan, 1976, 1987; Okay & Şahintürk, 1997; Kandemir & Yılmaz, 2009). The westernmost outcrop of the Kelkit Formation is in the western part of the Sakarya Zone in the Mudurnu region (Fig. 3; Altıner *et al.*, 1991; Genç & Tüysüz, 2010). Farther west, the Lower to Middle Jurassic consists of continental to shallow marine clastic rocks devoid of volcanism.

The Kelkit Formation lies unconformably over a heterogeneous Carboniferous or Triassic crystalline basement. It starts with coal-bearing sandstone, pebbly sandstone and conglomerate, which are locally overlain by Lower Jurassic (late Sinemurian-Pliensbachian, Bassoulet *et al.*, 1975; Meister & Alkaya, 1996; Vörös & Kandemir, 2011) Ammonitico Rosso levels. The Ammonitico Rosso type limestone and marl are overlain by a 2000 m thick sequence of lithic tuff, volcanogenic sandstone, shale, basaltic and andesitic lavas and conglomerate with rare coal and limestone horizons. There are also rare and small (up to a few kilometre-long) Lower–Middle Jurassic shallow-level granitic intrusions (Dokuz *et al.*, 2010).

Palynology of separate coal horizons in the Kelkit Formation gives Lower (Ağralı *et al.*, 1966; Pelin, 1977) and Middle Jurassic ages (Ağralı *et al.*, 1965). The presence of Middle Jurassic is further suggested by rare macrofossils (Wedding, 1963) and by the dinoflagellate and palynomorph assemblages (Robinson *et al.*, 1995). Thus, the age of the Kelkit Formation extends from late Sinemurian up to at least the end of Bathonian (190–165 Ma), and overlaps the metamorphism and plutonism in the Central Pontides.

The Kelkit Formation is conformably overlain by the Middle/Upper Jurassic–Lower Cretaceous shallow marine platform carbonates; the carbonate deposition starts earlier in the west in the Mudurnu area (Callovian, Altıner *et al.*, 1991) than in the Central-Eastern Pontides (Oxfordian/Kimmeridgian, Tunoğlu, 1992; Taşlı, 1993; Koch *et al.*, 2008; our unpublished information). Basaltic flows occur within the Upper Jurassic limestones (Pelin, 1977; Koçyiğit *et al.*, 1991; Taşlı, 1993; Koch *et al.*, 2008) indicating a gradual change from volcanism to carbonate deposition.

An extensional tectonic environment is unanimously accepted for the deposition of the Kelkit Formation. The evidence includes rapid lateral changes in thickness and facies interpreted to be due to syn-sedimentary normal faulting (Pelin, 1977; Görür *et al.*, 1983; Bergougnan, 1987; Koçyiğit *et al.*, 1991; Gürsoy, 1995; Kandemir & Yılmaz, 2009) and Neptunian dykes in the basement (Yılmaz & Kandemir, 2006; Kandemir & Yılmaz, 2009). The Kelkit Formation becomes finer grained and deeper marine south-

ward, suggesting that it was facing an ocean in the south (Okay & Şahintürk, 1997). Palaeomagnetic data from the Lower Jurassic Ammonitico Rosso limestone near the base of the Kelkit Formation (Channel *et al.*, 1996) and ammonite and brachiopod faunas (Meister & Alkaya, 1996; Vörös & Kandemir, 2011) indicate that the Kelkit Formation was deposited on the southern margin of Eurasia at a palaeolatitude of ~41°N, far north of Gondwana. Recently, Çinku (2011) obtained a palaeolatitude of ~30°N from the volcanic-volcanoclastic rocks of the Kelkit Formation, which for the Middle Jurassic (*c.* 160 Ma) also indicate a similar location.

The geochemistry of the volcanic rocks in the Kelkit Formation was studied by Şen (2007) and Genç & Tüysüz (2010). The volcanic rocks are all subalkaline and generally calcalkaline and range in composition from basalt to andesite. In the Mudurnu region, there are also subvolcanic dacite–porphyries (Genç & Tüysüz, 2010). The volcanic rocks show enrichment in LILEs and LREEs relative to HFSEs, and depletion in Nb, Ta, P and Ti, features typical for subduction-related magmas. Isotopic values of ϵNd and $^{87}\text{Sr}/^{86}\text{Sr}$ ratios also point to a magmatic arc setting (Genç & Tüysüz, 2010). The petrography and geochemistry of the sandstone in the Kelkit Formation also indicate deposition in a magmatic arc environment (Dokuz & Tanyolu, 2006). Thus, the stratigraphic and sedimentological features of the Kelkit Formation along with the geochemistry of the volcanic and sedimentary rocks indicate that the Kelkit Formation was deposited in extensional basins above a northward-dipping subduction zone.

Jurassic volcanic, volcanoclastic and clastic series in Crimea, Caucasus and Iran

The Lesser Caucasus constitutes the eastward extension of the Eastern Pontides (e.g. Yılmaz *et al.*, 2000). Jurassic volcanic sequences crop out widely both in the Greater and Lesser Caucasus with thicknesses locally of over 2000 m (Khain, 1975; Saintot *et al.*, 2006; McCann *et al.*, 2010; Adamia *et al.*, 2011). The northern margin of the Jurassic volcanism is sharply defined, and the Jurassic sequences on the northern flank of the Greater Caucasus (Fore Range zone) are devoid of volcanic rocks (Fig. 1, Rubin, 2007). The volcanism in the Caucasus started in the Early Jurassic but was especially extensive in the Middle Jurassic, and took place in an extensional to transtensional environment (Saintot *et al.*, 2006). The volcanic rocks range from basalt to rhyolite and their geochemistry generally shows a subduction signature; the volcanism is related to the northward subduction of the Tethys, which leads to formation of back-arc and intra-arc basins (Mengel *et al.*, 1987; McCann *et al.*, 2010). The absence of any Jurassic ophiolites in the Caucasus indicates that the extension did not result in the generation of oceanic lithosphere.

Jurassic magmatic rocks are also widely exposed in southeastern Crimea, and comprise lava flows, tuffs and small plutonic bodies, sills and feeder dykes within the pre-Upper Jurassic sedimentary sequences (Meijers *et al.*, 2010). The volcanic and subvolcanic rocks show similar geochemical features to those from the Central and Eastern Pontides. They range from basalt to dacite with a subalkaline to tholeiitic trend. The enrichment in LILEs, the low concentrations of Nb compared to the LILE and LREE are indicative of subduction-related magmas. Ar–Ar dating of plagioclase from the volcanic rocks gave Middle Jurassic (172–158 Ma) ages (Meijers *et al.*, 2010).

The Jurassic magmatic belt continues from Lesser Caucasus to Iran, where it is traced as a 1400 km long and ~70 km wide zone parallel and north of the Zagros suture (Fig. 1). The magmatic rocks consist of andesite, dacite and basalt and I-type granitoids with arc-type geochemistry (Berberian & King, 1981; Ahmadi Khalaji *et al.*, 2007; Omrani *et al.*, 2008; Chiu *et al.*, 2013). Zircon ages from the granitoid rocks are Middle to Late Jurassic (176–144 Ma) with a peak in the Middle Jurassic (Bathonian, *c.* 165 Ma, Chiu *et al.*, 2013), similar to those from the rest of the magmatic belt.

Magmatic arc setting for the Jurassic thermal event

Stratigraphic, faunal and palaeomagnetic data indicate that the Pontides were part of the active margin of Eurasia during the Jurassic (Enay, 1976; Channel *et al.*, 1996; Okay & Şahintürk, 1997). The West and East Black Sea basins are Cretaceous back-arc basins with oceanic or thinned continental crust (e.g. Okay *et al.*, 1994; Robinson *et al.*, 1996) and did not exist during the Jurassic. The restored Early–Middle Jurassic magmatic belt is ~100 km wide and extends for 2800 km from Crimea eastwards through the Pontides and the Caucasus to Iran. The westward termination of the Jurassic magmatic belt is well defined in northwest Turkey, where coeval sequences are free of magmatism (Fig. 1).

A magmatic arc origin has been generally accepted for the volcanic rocks in Caucasus, Crimea and Iran (Khain, 1975; Berberian & King, 1981; Saintot *et al.*, 2006; Meijers *et al.*, 2010; Adamia *et al.*, 2011; Nikişin *et al.*, 2012; Chiu *et al.*, 2013). On the other hand, Şengör & Yılmaz (1981) and Görür *et al.* (1983) suggested that the Jurassic volcanic rocks in the Pontides formed during the rifting of the Pontides from the Anatolide–Tauride Block. However, subsequent geochemical data showed a subduction rather than rift signature in the geochemistry of the Jurassic magmatic rocks in the Pontides (Şen, 2007; Genç & Tüysüz, 2010; this study). Furthermore, recent data from the İzmir–Ankara–Erzincan suture, including Triassic and Jurassic high- and medium-pressure metamorphic rocks (Okay & Monié, 1997; Çelik *et al.*, 2011; Okay *et al.*, 2013; Topuz *et al.*, 2013)

and Triassic radiolarian cherts in subduction-accretion complexes (Tekin & Gönçüoğlu, 2007), indicate the presence of a Triassic and older Tethyan ocean south of the Pontides. Middle Jurassic (170–161 Ma) high-pressure amphibolite facies metabasite and micaschist crop out over large areas in the southern part of the Central Pontides (Fig. 3), and are interpreted as a subduction-accretion complex (Okay *et al.*, 2013). Thus during the Jurassic, Pontides constituted part of the Eastern Black Sea magmatic arc, as initially suggested by Yılmaz & Boztuğ (1986).

The Jurassic volcanism in the Pontides was submarine and the lavas are interbedded with volcanoclastic rocks, sandstones, shales and locally limestones with an aggregate thickness reaching to 2000 m. This, together with syn-sedimentary normal faulting and Neptunian dykes show that the arc was extensional with intra-arc basins separated by volcanic centres. It was similar to the Cretaceous magmatic arc of the Eastern Pontides (cf. Okay & Şahintürk, 1997).

METAMORPHISM AND MAGMATISM DURING EXTENSION

Several lines of evidence, summarized below, indicate that the Jurassic magmatism and metamorphism occurred in an extensional magmatic arc setting in the Central Pontides and in the Black Sea region in general.

- 1 An ~2 km thick Lower–Middle Jurassic volcanoclastic and volcanic sequence crops out in the Central and Eastern Pontides. The rapid lateral facies and thickness changes, submarine nature of the volcanism, presence of syn-sedimentary normal faulting and Neptunian dykes within this sequence indicate deposition in an extensional setting.
- 2 There is no evidence for a Jurassic contractional deformation affecting the Lower–Middle Jurassic series in the Pontides. The Lower–Middle Jurassic volcanic-rich sequence is overlain by Upper Jurassic carbonates with intercalated lava flows and with no evidence of an intervening Jurassic deformation. The Alpidic deformation in the Central and Eastern Pontides started in the Early Cretaceous (Albian).
- 3 The Middle Jurassic metamorphism and plutonism were coeval with submarine sedimentation and volcanism showing that there was no ongoing crustal thickening during the metamorphism.
- 4 The sedimentation in the Pontides started in the Early Jurassic (Pliensbachian, *c.* 185 Ma) indicating that there was no crustal thickening preceding Middle Jurassic metamorphism.
- 5 There is no petrological evidence for a previous higher pressure metamorphism in the metamorphic rocks.

The presence of unmetamorphosed Triassic and older sedimentary sequences in the vicinity of the Jurassic metamorphic rocks (Fig. 3) indicates that

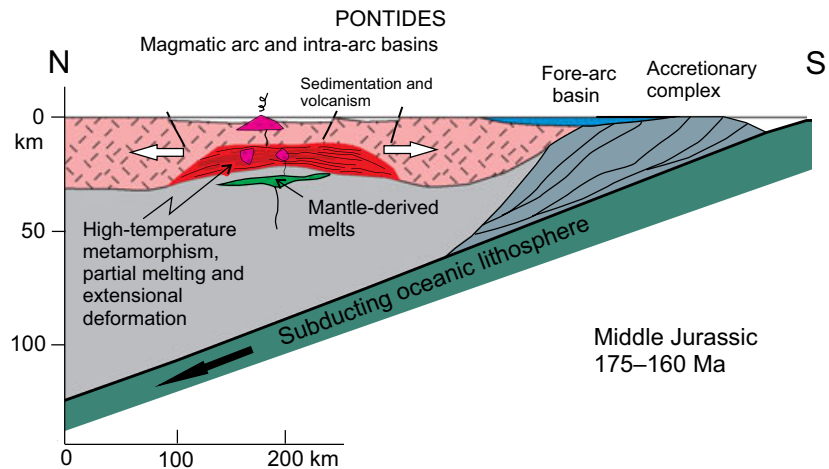


Fig. 17. Schematic model showing an extensional magmatic arc tectonic setting for the Middle Jurassic metamorphism and magmatism in the Central Pontides.

heat flow was focused and transient, and the thermal gradients were high, which is compatible with a setting in the mid-levels of a continental magmatic arc.

In contrast to many regions of LP-HT metamorphism, where there is evidence for previous crustal thickening (e.g. Amato *et al.*, 1994; Platt *et al.*, 2003), the regional stratigraphy and the petrography of the metamorphic rocks in the Central Pontides indicate that there was no crustal thickening prior to Early–Middle Jurassic extension and metamorphism. The extension was most probably caused by the roll-back of the subduction oceanic slab, as in the case of the Aegean Sea (e.g. Jolivet *et al.*, 2013).

In the preferred model, the extension and associated metamorphism and magmatism in the Central Pontides occur in the mid-crustal levels of a continental magmatic arc developed above the northward subducting oceanic lithosphere (Fig. 17). Heat is transported upwards in the crust by mantle-derived magmas, which resulted in partial melting of the mid-crust under the magmatic arc. Evidence for an early mafic magmatism is found in the dioritic, gabbroic and ultramafic enclaves in the Karaman Pluton. The magmatic arc is under extension due to slab roll-back, and the submarine volcanism and sedimentation are controlled by normal faulting. The sedimentation on the surface is coeval with high-temperature metamorphism and migmatitization at 15 km depth. The convective heat is focused under the arc, and neighbouring regions are not affected by the high-temperature metamorphism, as illustrated by the unmetamorphosed Triassic sequences in the region.

There are few data on the exhumation mechanism of the high-temperature metamorphic rocks in the Central Pontides since most of their contacts are unconformably covered by the Lower Cretaceous turbidites. The exhumation must have occurred during ongoing magmatism as the metamorphic rocks formed at 15 km depth at *c.* 172 Ma are intruded by upper crustal porphyries, emplaced probably at

3–5 km depth, in the Middle Jurassic (*c.* 163 Ma). The high-temperature metamorphic rocks and migmatite could have risen in the crust as diapirs during ongoing crustal melting (e.g. Teyssier & Whitney, 2002), as suggested for example for the Kigluak gneiss dome in Alaska (Amato *et al.*, 1994).

CONCLUSIONS

Jurassic metamorphism in the Central Pontides is a low pressure–high temperature type with the characteristic mineral assemblage of quartz + K-feldspar + plagioclase + biotite + cordierite ± sillimanite ± garnet in the gneiss. The estimated peak *P–T* conditions of the metamorphism are 4 ± 1 kbar and 720 ± 40 °C. The U–Pb zircon and Ar–Ar biotite data indicate that the peak metamorphism occurred during the Middle Jurassic at *c.* 172 Ma and the rocks cooled to 300 °C at 164 Ma.

The Jurassic metamorphic rocks are associated with a series of Middle Jurassic calcalkaline shallow-level intrusions represented mainly by porphyries. The presence of cordierite and garnet and abundant inherited zircon in the porphyries indicate a major crustal melt component in their formation. New Ar–Ar biotite data indicate Middle Jurassic ages (163 and 162 Ma) for two of these intrusions. Geochemical data from the porphyries and the volcanic rocks indicate formation in a magmatic arc.

The Jurassic magmatic rocks form a west to south-east trending belt extending from the Central Pontides through Crimea and Caucasus to Iran. The regional tectonic setting and the geochemistry suggest a magmatic arc setting.

The following arguments indicate that the LP-HT metamorphism occurred at the deep levels of an extensional Jurassic magmatic arc. (i) Metamorphism is of low pressure–high temperature type and is associated with partial melting. (ii) The associated magmatic rocks have geochemical signatures indicating a magmatic arc setting. (iii) The Jurassic metamor-

phism and associated magmatism are restricted in space and time. The Triassic Küre Complex, a few kilometres east of the Jurassic metamorphic belt, shows no evidence of metamorphism. (iv) There is no evidence for Middle Jurassic contractional deformation in the Central Pontides or in the Black Sea region. (v) The coeval Jurassic volcanic rocks in the Black Sea region occur within thick clastic and volcanoclastic sequences deposited in extensional basins, as shown by syn-sedimentary normal faulting and Neptunian dykes.

The preferred tectonic setting of the metamorphism involves, mantle-derived magmas in a magmatic arc emplaced below an extending lower crust. The mafic magmas lead to high-temperature metamorphism and crustal melting at depths of 10–15 km (Fig. 17). The high-temperature metamorphic rocks and migmatite rise diapirically to upper crustal levels (3–5 km), where they are intruded by crustal melts, represented by the Middle Jurassic porphyries.

ACKNOWLEDGEMENTS

This study was supported by TÜBİTAK grant 109Y049, İTÜ BAP 33342 and partly by TÜBA. We thank S.C. Ülgen and R. Akdoğan for helping in the mineral separation, H-P. Schertl and H-J. Bernhardt for use of the electron microprobe, E. Aydar and E. Çubukçu for help with the cathodoluminescence images of zircon, A. Halton and J. Malley for helping in analysing the samples for Ar/Ar dating. O. Candan and D. Whitney are thanked for their comments, which improved the manuscript.

REFERENCES

- Adamia, S., Zakariadze, G., Chkhotua, T. *et al.*, 2011. Geology of the Caucasus: A review. *Turkish Journal of Earth Sciences*, **20**, 489–544.
- Ağralı, B., Akyol, E. & Konyalı, Y., 1965. Preuves palynologiques de l'existence du Dogger dans la région de Bayburt. *Bulletin of the Mineral Research and Exploration Institute of Turkey*, **65**, 45–57.
- Ağralı, B., Akyol, E. & Konyalı, Y., 1966. Palynological study of three coal horizon in the Jurassic of Kelkit-Bayburt. *Türkiye Jeoloji Kurumu Bülteni*, **10**, 149–155 (in Turkish).
- Ahmadi Khalaji, A., Esmaily, D., Valizadeh, M.V. & Rahimpour-Bonab, H., 2007. Petrology and geochemistry of the granitoid complex of Boroujerd, Sanandaj-Sirjan Zone, Western Iran. *Journal of Asian Earth Sciences*, **29**, 859–877.
- Altner, D., Koçyiğit, A., Farinacci, A., Nicosia, U. & Conti, M.A., 1991. Jurassic-Lower Cretaceous stratigraphy and paleogeographic evolution of the southern part of north-western Anatolia. *Geologica Romana*, **28**, 13–80.
- Altun, I., Şengün, M., Keskin, H. *et al.*, 1990. *Geological Map of the Kastamonu Region, 1/100 000 Scale*. Maden Tetkik ve Arama Genel Müdürlüğü, Ankara.
- Amato, J.A., Wright, J.E., Gans, P.B. & Miller, E.L., 1994. Magmatically induced metamorphism and deformation in the Kigluaik gneiss dome, Seward Peninsula, Alaska. *Tectonics*, **13**, 515–527.
- Aydın, M., Demir, O., Özçelik, Y., Terzioğlu, N. & Satır, M., 1995. A geological revision of Inebolu, Devrekani, Ağlı and Küre areas: New observations in Paleo-Tethys – Neo-Tethys sedimentary successions. In: *Geology of the Black Sea Region* (eds Erler, A., Ercan, T., Bingöl, E. & Orçen, S.), pp. 33–38. Maden Tetkik ve Arama Genel Müdürlüğü, Ankara.
- Barton, M.D. & Hanson, R.B., 1989. Magmatism and the development of low-pressure metamorphic belts: Implications from the western United States and thermal modeling. *Geological Society of America Bulletin*, **101**, 1051–1065.
- Bassoulet, J.-P., Bergougnan, H. & Enay, R., 1975. Répartition des faunes et faciès liasiques dans l'Est de la Turquie, région du Haut-Euphrate. *Comptes rendus de l'Académie des Sciences*, **280**, 583–586.
- Berberian, M. & King, G., 1981. Toward a paleogeography and tectonic evolution of Iran. *Canadian Journal of Earth Sciences*, **18**, 210–265.
- Bergougnan, H., 1976. Structure de la Chaîne pontique dans le Haut-Kelkit (Nord-Est de l'Anatolie). *Bulletin de la Société géologique de France*, **13**, 675–686.
- Bergougnan, H., 1987. *Etudes géologiques dans l'est-Anatolien*. PhD thesis, University Pierre et Marie Curie, Paris, France, 606 pp.
- Boynton, W.V., 1984. Geochemistry of the rare earth elements: meteorite studies. In: *Rare Earth Element Geochemistry* (ed Henderson, P.), pp. 63–114. Elsevier, Amsterdam.
- Boztaş, D., 1992. Petrography of the magmatic-metamorphic rocks and the major element chemistry of the magmatic rocks in the Küre region, west-central Pontides (in Turkish). *Cumhuriyet Üniversitesi, Mühendislik Fakültesi Dergisi, Seri-A, Yerbilimleri*, **9**, 75–106.
- Boztaş, D., Debon, F., Le Fort, P. & Yılmaz, O., 1995. High compositional diversity of the Middle Jurassic Kastamonu Plutonic Belt, northern Anatolia, Turkey. *Turkish Journal of Earth Sciences*, **4**, 67–86.
- Bragin, N.Y., Tekin, U.K. & Özçelik, Y., 2002. Middle Jurassic radiolarians from the Akgöl formation, central Pontids, northern Turkey. *Neues Jahrbuch für Geologie und Paläontologie, Monatshefte*, **2002**, 609–628.
- Çelik, Ö.F., Marzoli, A., Marschik, R., Chiaradia, M., Neubauer, F. & Öz, İ., 2011. Early–Middle Jurassic intra-oceanic subduction in the Izmir-Ankara-Erzincan Ocean, Northern Turkey. *Tectonophysics*, **539**, 120–134.
- Channel, J.E.T., Tüysüz, O., Bektas, O. & Sengör, A.M.C., 1996. Jurassic-Cretaceous paleomagnetism and paleogeography of the Pontides (Turkey). *Tectonics*, **15**, 201–212.
- Chen, F., Siebel, W., Satır, M., Terzioğlu, N. & Saka, K., 2002. Geochronology of the Karadere basement (NW Turkey) and implications for the geological evolution of the Istanbul Zone. *International Journal of Earth Sciences*, **91**, 469–481.
- Chiu, H.-Y., Chung, S.-L., Zarrinkoub, M.H., Mohammadi, S.S., Khatib, M.M. & Iizuka, Y., 2013. Zircon U-Pb age constraints from Iran on the magmatic evolution related to Neotethyan subduction and Zagros orogeny. *Lithos*, **162–163**, 70–87.
- Çinku, M.C., 2011. Paleogeographic evidence on the Jurassic tectonic history of the Pontides: New paleomagnetic data from the Sakarya continent and Eastern Pontides. *International Journal of Earth Sciences*, **100**, 1633–1645.
- Craven, S.J., Daczko, N.R. & Halpin, J.A., 2012. Thermal gradient and timing of high-T–low-P metamorphism in the Wongwibinda Metamorphic Complex, southern New England Orogen, Australia. *Journal of Metamorphic Geology*, **30**, 3–20.
- Dean, W.T., Monod, O., Rickards, R.B., Demir, O. & Bul-tynck, P., 2000. Lower Palaeozoic stratigraphy and palaeontology, Karadere-Zirze area, Pontus Mountains, northern Turkey. *Geological Magazine*, **137**, 555–582.
- Derman, A.S., Alişan, C. & Özçelik, Y., 1995. Himmetpaşa formation: A new palynological age and stratigraphic significance. In: *Geology of the Black Sea Region* (eds Erler, A., Ercan, T., Bingöl, E. & Orçen, S.), pp. 99–103. Maden Tetkik ve Arama Enstitüsü, Ankara.

- Deyoreo, J.J., Lux, D.R. & Guidotti, C.V., 1991. Thermal modeling in low-pressure high-temperature metamorphic belts. *Tectonophysics*, **188**, 209–238.
- Dokuz, A. & Tanyolu, E., 2006. Geochemical constraints on the provenance, mineral sorting and subaerial weathering of Lower Jurassic and Upper Cretaceous clastic rocks of the Eastern Pontides, Yusufeli (Artvin), NE Turkey. *Turkish Journal of Earth Sciences*, **15**, 181–209.
- Dokuz, A., Karlı, O., Chen, B. & Uysal, I., 2010. Sources and petrogenesis of Jurassic granitoids in the Yusufeli area, Northeastern Turkey: Implications for pre- and post-collisional lithospheric thinning of the eastern Pontides. *Tectonophysics*, **480**, 258–279.
- Enay, R., 1976. Faunes Anatoliennes (Ammonitina, Jurassique) et domaines biogéographiques nord et sud Téthysiens. *Bulletin de la Société géologique de France*, **18**, 533–541.
- Gardien, V., Lardeaux, J.M., Ledru, P., Allemand, P. & Guillot, S., 1997. Metamorphism during late orogenic extension: Insights from the French Variscan belt. *Bulletin de la Société Géologique de France*, **168**, 271–286.
- Genç, Ş.C. & Tüysüz, O., 2010. Tectonic setting of the Jurassic bimodal magmatism in the Sakarya Zone (Central and Western Pontides), Northern Turkey: A geochemical and isotopic approach. *Lithos*, **118**, 95–111.
- Görür, N., Şengör, A.M.C., Akkök, R. & Yılmaz, Y., 1983. Sedimentological data regarding the opening of the northern branch of the Neo-Tethys (in Turkish). *Türkiye Jeoloji Kurumu Bülteni*, **26**, 11–19.
- Görür, N., Monod, O., Okay, A.I. *et al.*, 1997. Palaeogeographic and tectonic position of the Carboniferous rocks of the western Pontides (Turkey) in the frame of the Variscan belt. *Bulletin de la Société Géologique de France*, **168**, 197–205.
- Gürsoy, H., 1995. The main tectonic structures of the Kelkit (Gümüşhane) region and their relationship with the regional tectonic structures, NE Turkey. In: *Geology of the Black Sea Region* (eds Erler, A., Ercan, T., Bingöl, E. & Orçen, S.), pp. 292–299. Maden Tetkik ve Arama Genel Müdürlüğü, Ankara.
- Harrison, T.M., Duncan, I. & McDougall, I., 1985. Diffusion of Ar-40 in biotite – Temperature, pressure and compositional effects. *Geochimica et Cosmochimica Acta*, **49**, 2461–2468.
- Hippolyte, J.-C., Müller, C., Kaymakçı, N. & Sangu, E., 2010. Dating of the Black Sea Basin: New nannoplankton ages from its inverted margin in the Central Pontides (Turkey). In: *Sedimentary Basin Tectonics from the Black Sea and Caucasus to the Arabian Platform* (eds Stephenson, R. A., Kaymakci, N., Sosson, M., Starostenko, V. & Bergerat, F.), *Geological Society, London, Special Publication*, **340**, 113–136.
- Holland, T.J.B. & Powell, R., 1998. An internally consistent thermodynamic data set for phases of petrological interest. *Journal of Metamorphic Geology*, **16**, 309–343.
- Irvine, T.N. & Barager, W.R.A., 1971. Chemical differentiation of the Earth: The relationship between mantle, continental crust and oceanic crust. *Canadian Journal of Earth Sciences*, **8**, 523–543.
- Jolivet, L., Faccenna, C., Huet, B. *et al.*, 2013. Aegean tectonics: Strain localisation, slab tearing and trench retreat. *Tectonophysics*, **597–598**, 1–33.
- Kandemir, R. & Yılmaz, C., 2009. Lithostratigraphy, facies, and deposition environment of the lower Jurassic Ammonitico Rosso type sediments (ARTS) in the Gumuşhane area, NE Turkey: Implications for the opening of the northern branch of the Neo-Tethys Ocean. *Journal of Asian Earth Sciences*, **34**, 586–598.
- Khain, V.E., 1975. Structure and main stages in the tectono-magmatic development of the Caucasus: An attempt at geodynamic interpretation. *American Journal of Science*, **275-A**, 131–156.
- Koch, R., Bucur, I.I., Kirmaci, M.Z., Eren, M. & Tasli, K., 2008. Upper Jurassic and Lower Cretaceous carbonate rocks of the Berdiga Limestone – Sedimentation on an onbound platform with volcanic and episodic siliciclastic influx. Biostratigraphy, Facies and Diagenesis (Kircaova, Kale-Gümüşhane area; NE-Turkey). *Neues Jahrbuch für Geologie und Paläontologie*, **247**, 23–61.
- Koçyiğit, A., Altıner, D., Farinacci, A., Nicosia, U. & Conti, M.A., 1991. Late Triassic-Aptian evolution of the Sakarya divergent margin: Implications for the opening history of the northern Neo-Tethys, in north-western Anatolia, Turkey. *Geologica Romana*, **28**, 81–99.
- Lucassen, F. & Franz, G., 1996. Magmatic arc metamorphism: Petrology and temperature history of metabasic rocks in the Coastal Cordillera of northern Chile. *Journal of Metamorphic Geology*, **14**, 249–265.
- Maden Tetkik ve Arama Enstitüsü, 1974. *Geological Map of the Zonguldak E29-a-b-c-d, Kastamonu E30a-b Sheets, 1:50 000 scale*. Maden Tetkik ve Arama Enstitüsü, Ankara.
- McCann, T., Chalot-Prat, F. & Saintot, A., 2010. The Early Mesozoic evolution of the Western Greater Caucasus (Russia): Triassic-Jurassic sedimentary and magmatic history. In: *Sedimentary Basin Tectonics from the Black Sea and Caucasus to the Arabian Platform* (eds Sosson, M., Kaymakci, N., Stephenson, R. A., Bergerat, F. & Starostenko, V.), *Geological Society of London, Special Publication*, **340**, 181–238.
- Meijers, M.J.M., Vrouwe, B., van Hinsbergen, D.J.J. *et al.*, 2010. Jurassic arc volcanism on Crimea (Ukraine): Implications for the paleo-subduction zone configuration of the Black Sea region. *Lithos*, **119**, 412–426.
- Meister, C. & Alkaya, F., 1996. Ammonite biostratigraphy of the Sinemurian-Pliensbachian in central and eastern Pontides (Turkey): Preliminary remarks. In: *Advances in Jurassic Research* (ed. Riccardi, A.C.), *Georesearch Forum*, **1–2**, 129–134.
- Mengel, K., Borsuk, A.M., Gurbanov, A.G., Wedepohl, K.H. & Hoefs, J., 1987. Origin of spilitic rocks from the southern slope of the Greater Caucasus. *Lithos*, **20**, 115–133.
- Nikishin, A., Ziegler, P., Bolotov, S. & Fokin, P., 2012. Late Palaeozoic to Cenozoic evolution of the Black Sea-Southern Eastern Europe region: A view from the Russian Platform. *Turkish Journal of Earth Sciences*, **21**, 571–634.
- Nzegge, O. M., 2007. *Petrogenesis and geochronology of the Deliklitas, Sivrikaya and Devrekani granitoids and basement, Kastamonu belt–Central Pontides (NW Turkey): Evidence for Late Palaeozoic-Mesozoic plutonism and geodynamic interpretation*. PhD thesis, University of Tübingen, 167 pp.
- Nzegge, O.M., Satir, M., Siebel, W. & Taubald, H., 2006. Geochemical and isotopic constraints on the genesis of the Late Palaeozoic Deliklitas, and Sivrikaya granites from the Kastamonu granitoid belt (Central Pontides, Turkey). *Neues Jahrbuch für Geologie und Paläontologie*, **183**, 27–40.
- Okay, A.I. & Monié, P., 1997. Early Mesozoic subduction in the Eastern Mediterranean: Evidence from Triassic eclogite in northwest Turkey. *Geology*, **25**, 595–598.
- Okay, A.I. & Şahintürk, Ö., 1997. Geology of the Eastern Pontides. In: *Regional and Petroleum Geology of the Black Sea and Surrounding Region* (ed. Robinson, A.G.). *American Association of Petroleum Geologists (AAPG) Memoir*, **68**, 291–311.
- Okay, A.I. & Tüysüz, O., 1999. Tethyan sutures of northern Turkey. In: *The Mediterranean Basins: Tertiary Extension within the Alpine Orogen* (eds Durand, B., Jolivet, L., Horváth, F. & Séranne, M.), *Geological Society of London, Special Publication*, **156**, 475–515.
- Okay, A.I., Şengör, A.M.C. & Görür, N., 1994. Kinematic history of the opening of the Black Sea and its effects on the surrounding regions. *Geology*, **22**, 267–270.
- Okay, A.I., Tüysüz, O., Satir, M. *et al.*, 2006. Cretaceous and Triassic subduction-accretion, HP/LT metamorphism and continental growth in the Central Pontides, Turkey. *Geological Society of America Bulletin*, **118**, 1247–1269.
- Okay, A.I., Sunal, G., Sherlock, S. *et al.*, 2013. Early Cretaceous sedimentation and orogeny on the southern active margin of Eurasia: Central Pontides, Turkey. *Tectonics*, **32**, 1247–1271.

- Omranı, C., Agard, P., Whitechurch, H., Benoit, M., Prouteau, G. & Jolivet, L., 2008. Arc-magmatism and subduction history beneath the Zagros Mountains, Iran: A new report of adakites and geodynamic consequences. *Lithos*, **106**, 380–398.
- Özgül, N., 2012. Stratigraphy and some structural features of the Istanbul Palaeozoic. *Turkish Journal of Earth Sciences*, **21**, 817–866.
- Pearce, J.A., 1983. Role of the sub-continental lithosphere in magma genesis at active continental margins. In: *Continental Basalts and Mantle Xenolites* (eds Hawkesworth, C.J. & Norry, M.J.), pp. 230–249. Shiva, Nantwich.
- Pearce, J.A., 1996. A user's guide to basalt discrimination diagrams. In: *Trace Element Geochemistry of Volcanic Rocks: Applications for Massive Sulphide Exploration* (ed. Wyman, D.A.), *Geological Association of Canada, Short Course Notes*, **12**, 79–113.
- Pearce, J.A. & Peate, D.W., 1995. Tectonic implications of the composition of volcanic arc magmas. *Annual Review of the Earth and Planetary Sciences*, **23**, 113–134.
- Pearce, J.A., Harris, N.B.W. & Tindle, A.G., 1984. Trace-element discrimination diagrams for the tectonic interpretation of granitic-rocks. *Journal of Petrology*, **25**, 956–983.
- Pelin, S., 1977. Geological Study of the Area southeast of Alucra (Giresun) with Special Reference to its Petroleum Potential (in Turkish). Karadeniz Teknik Üniversitesi Publication, No. 87, Trabzon, 103 pp.
- Platt, J.P., Whitehouse, M.J., Kelley, S.P., Carter, A. & Hollick, L., 2003. Simultaneous extensional exhumation across the Alboran Basin: Implications for the causes of late orogenic extension. *Geology*, **31**, 251–254.
- Powell, R. & Holland, T.J.B., 1988. An internally consistent thermodynamic dataset with uncertainties and correlations: 3. Application methods, worked examples and a computer program. *Journal of Metamorphic Geology*, **6**, 173–204.
- Robinson, A.G., Banks, C.J., Rutherford, M.M. & Hirst, J.P.P., 1995. Stratigraphic and structural development of the Eastern Pontides, Turkey. *Journal of the Geological Society, London*, **152**, 861–872.
- Robinson, A.G., Rudat, J.H., Banks, C.J. & Wiles, R.L.F., 1996. Petroleum geology of the Black Sea. *Marine and Petroleum Geology*, **13**, 195–223.
- Rollinson, H., 1993. *Using Geochemical Data: Evaluation, Presentation, Interpretation*. Longman Group, Harlow, England, 352 pp.
- Rubin, D.A., 2007. Jurassic transgressions and regressions in the Caucasus (northern Neotethys Ocean) and their influences on the marine biodiversity. *Palaeogeography, Palaeoclimatology, Palaeoecology*, **251**, 422–436.
- Saintot, A., Brunet, M-F., Yakovlev, F. et al., 2006. The Mesozoic-Cenozoic tectonic evolution of the Greater Caucasus. In: *European Lithosphere Dynamics* (eds Gee, D.G. & Stephenson, R.A.), *Geological Society of London, Memoir*, **32**, 277–289.
- Şen, C., 2007. Jurassic volcanism in the Eastern Pontides: Is it rift related or subduction related? *Turkish Journal of Earth Sciences*, **16**, 523–539.
- Şengör, A.M.C. & Yılmaz, Y., 1981. Tethyan evolution of Turkey: A plate tectonic approach. *Tectonophysics*, **75**, 181–241.
- Şengör, A.M.C., Cin, A., Rowley, D.B. & Nie, S.Y., 1991. Magmatic evolution of the Tethysides: A guide to reconstruction of collage history. *Palaeogeography, Palaeoclimatology, Palaeoecology*, **87**, 411–440.
- Streckeisen, A., 1976. To each plutonic rock its proper name. *Earth Science Reviews*, **12**, 1–33.
- Sun, S.S. & McDonough, W.F., 1989. Chemical and isotopic systematics of oceanic basalts: Implications for mantle composition and processes. In *Magmatism in Ocean Basins* (eds Saunders, A.D. & Norry, M.J.), *Geological Society, London, Special Publication*, **42**, 313–345.
- Tash, K., 1993. Micropaléontologie, stratigraphie et environnement de dépôt des séries Jurassiques a faciès de plat-forme de la région de Kale-Gümüşhane (Pontides Orientales, Turquie). *Revue de Micropaléontologie*, **36**, 45–65.
- Taylor, S.R. & McLennan, S.M., 1985. *The Continental Crust: Its Composition and Evolution*. Geoscience Texts, Blackwell Scientific Publications, London, 312 pp.
- Tekin, U.K. & Göncüoğlu, M.C., 2007. Discovery of the oldest (Upper Ladinian to Middle Carnian) radiolarian assemblages from the Bornova Flysch Zone in western Turkey: Implications for the evolution of the Neotethyan Izmir-Ankara ocean. *Ofoliti*, **32**, 131–150.
- Teyssier, C. & Whitney, D.L., 2002. Gneiss domes and orogeny. *Geology*, **30**, 1139–1142.
- Topuz, G., Göcmengil, G., Rolland, Y., Çelik, Ö.F., Zack, T. & Schmitt, A.K., 2013. Jurassic accretionary complex and ophiolite from northeast Turkey: No evidence for the Cimmerian continental ribbon. *Geology*, **41**, 255–258.
- Tunoğlu, C., 1992. Microfacies analysis in the Upper Jurassic–Lower Cretaceous carbonates sequence of the Devrekani Basin (north of Kastamonu) (in Turkish). *Türkiye Petrol Jeologları Derneği Bülteni*, **3**, 75–86.
- Tüysüz, O., 1990. Tectonic evolution of a part of the Tethyside orogenic collage: The Kargı Massif, northern Turkey. *Tectonics*, **9**, 141–160.
- Tüysüz, O., 1999. Geology of the Cretaceous sedimentary basins of the Western Pontides. *Geological Journal*, **34**, 75–93.
- Tüysüz, O., Keskin, M., Natalin, B. & Sunal, G., 2000. *Geology of the Inebolu-Ağlı-Azdavay Region (in Turkish)*. Internal Report of the Turkish Petroleum Corporation, No. 4250, 240 pp. (unpublished).
- Uğuz, M.F., Sevin, M. & Duru, M., 2002. *Geological Map of Turkey, Sinop Sheet, 1: 500 000 Scale*. Maden Tetkik ve Arama (MTA) Genel Müdürlüğü, Ankara.
- Ustaömer, T. & Robertson, A.H.F., 1993. A Late Paleozoic-Early Mesozoic marginal basin along the active southern continental margin of Eurasia: Evidence from the Central Pontides (Turkey) and adjacent regions. *Geological Journal*, **28**, 219–238.
- Ustaömer, T. & Robertson, A.H.F., 1994. Late Palaeozoic marginal basin and subduction-accretion: The Paleotethyan Küre Complex, Central Pontides, northern Turkey. *Journal of the Geological Society, London*, **151**, 291–305.
- Ustaömer, T. & Robertson, A.H.F., 1999. Geochemical evidence used to test alternative plate tectonic models for the pre-Upper Jurassic (Palaeotethyan) units in the Central Pontides, N Turkey. *Geological Journal*, **34**, 25–53.
- Vissers, R.L.M., 1992. Variscan extension in the Pyrenees. *Tectonics*, **11**, 1369–1384.
- Vörös, A. & Kandemir, R., 2011. A new Early Jurassic brachiopod fauna from the Eastern Pontides (Turkey). *Neues Jahrbuch für Geologie und Paläontologie*, **260**, 343–363.
- Wedding, H., 1963. Beiträge zur Geologie der Kelkitlinie und zur Stratigraphie des Jura im Gebiet Kelkit-Bayburt (Gümüşhane). *Bulletin of the Mineral Research and Exploration Institute of Turkey*, **61**, 31–37.
- Wickham, S.M. & Oxburgh, E.R., 1985. Continental rifts as a setting for regional metamorphism. *Nature*, **318**, 330–333.
- Winchester, J.A. & Floyd, P.A., 1977. Geochemical discrimination of different magma series and their differentiation products using immobile elements. *Chemical Geology*, **20**, 325–343.
- Yığıtbaş, E., Elmas, A. & Yılmaz, Y., 1999. Pre-Cenozoic tectono-stratigraphic components of the Western Pontides and their geological evolution. *Geological Journal*, **34**, 55–74.
- Yılmaz, O., 1980. Tectonics and lithostratigraphic units of the northeastern part of the Daday-Devrekani massif (in Turkish). *Yerbilimleri*, **5–6**, 101–135.
- Yılmaz, O., 1981. Petrography and whole rock chemistry of the Ebrek Metamorphite of the Daday-Devrekani Massif, western Pontides, Turkey (in Turkish). *Yerbilimleri*, **8**, 71–82.
- Yılmaz, O., 1988. L'ensemble ophiolitique de Çangal (Turquie du Nord): Mise en évidence d'un métamorphisme océanique

- et d'un rétro-métamorphisme cataclastique tardif. *Geologie Alpine*, **64**, 113–132.
- Yılmaz, O. & Boztuğ, D., 1986. Kastamonu granitoid belt of northern Turkey: First arc plutonism product related to the subduction of the Paleo-Tethys. *Geology*, **14**, 179–183.
- Yılmaz, C. & Kandemir, R., 2006. Sedimentary records of the extensional tectonic regime with temporal cessation: Gümüşhane Mesozoic basin (NE Turkey). *Geologica Carpathica*, **57**, 3–13.
- Yılmaz, Y. & Şengör, A.M.C., 1985. Palaeo-Tethyan ophiolites in northern Turkey: Petrology and tectonic setting. *Ofoliti*, **10**, 485–504.
- Yılmaz, Y., Tüysüz, O., Yiğitbaş, E., Genç, C.Ş. & Şengör, A.M.C., 1997. Geology and tectonic evolution of the Pontides. In: *Regional and Petroleum Geology of the Black Sea and Surrounding Region* (ed. Robinson, A.G.), *American Association of Petroleum Geologists Memoir*, **68**, 183–226.
- Yılmaz, A., Adamia, S., Chabukiani, A. *et al.*, 2000. Structural correlation of the southern Transcaucasus (Georgia) – Eastern Pontides (Turkey). In: *Tectonics and Magmatism in Turkey and Surrounding Area* (eds Bozkurt, E., Winchester, J.A. & Piper, J.A.D.), *Geological Society of London, Special Publication*, **173**, 171–182.

SUPPORTING INFORMATION

Additional Supporting Information may be found in the online version of this article at the publisher's web site:

Appendix S1. Methods employed during electron microprobe, Ar–Ar, U–Pb and geochemical analyses.

Table S1. Ar–Ar isotopic data from the metamorphic and magmatic rocks.

Table S2. U–Pb zircon isotopic data from the metamorphic and magmatic rocks.

Table S3. Geochemical data.

Received 30 June 2013; revision accepted 22 October 2013.